New Experiments to Measure the Muon Anomalous Gyromagnetic Ratio

Michael Eads
Northern Illinois University

Introduction

Magnetic Moments

- For a point particle, the magnetic moment is proportional to the charge, mass, spin, and a proportionality factor, *g*

$$\overrightarrow{\mu} = g\frac{e}{2m}\overrightarrow{s}$$

- For spin-1/2 particle, *g* close to 2. Often expressed as anomalous magnetic moment:

$$a = \frac{g-2}{2}$$

Why muons?

- Excellent agreement for electrons

PRL **100**, 120801 (2008). $$a_e^{exp} = 1\ 159\ 652\ 180.73(28) \times 10^{-12}$$

PRL **109**, 111807 (2012). $$a_e^{th} = 1\ 159\ 652\ 181.78(77) \times 10^{-12}$$

$$\Rightarrow \boxed{\Delta a_e = (1.05 \pm 0.82) \times 10^{-12}}$$

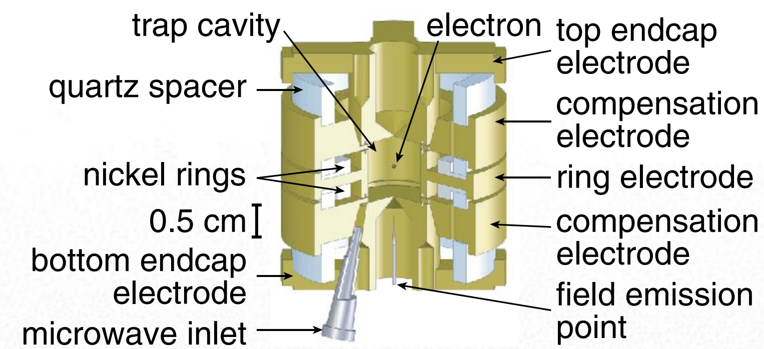

FIG. 2 (color). Cylindrical Penning trap cavity used to confine a single electron and inhibit spontaneous emission.

- Agreement is to part-per-trillion level!
- Muons the only other charged spin-1/2 point particle that are “stable”
- Naive mass scaling suggests muons may be more sensitive to new physics effects coming from loops

Standard Model Prediction for a_μ

- QED (a) contribution by far the largest, but has very small uncertainty (calculated to 5 loops)
- Weak contribution (b) also well known (calculated to 3 loops)
- Uncertainty dominated by hadronic vacuum polarization (c) and hadronic light-by-light (d)

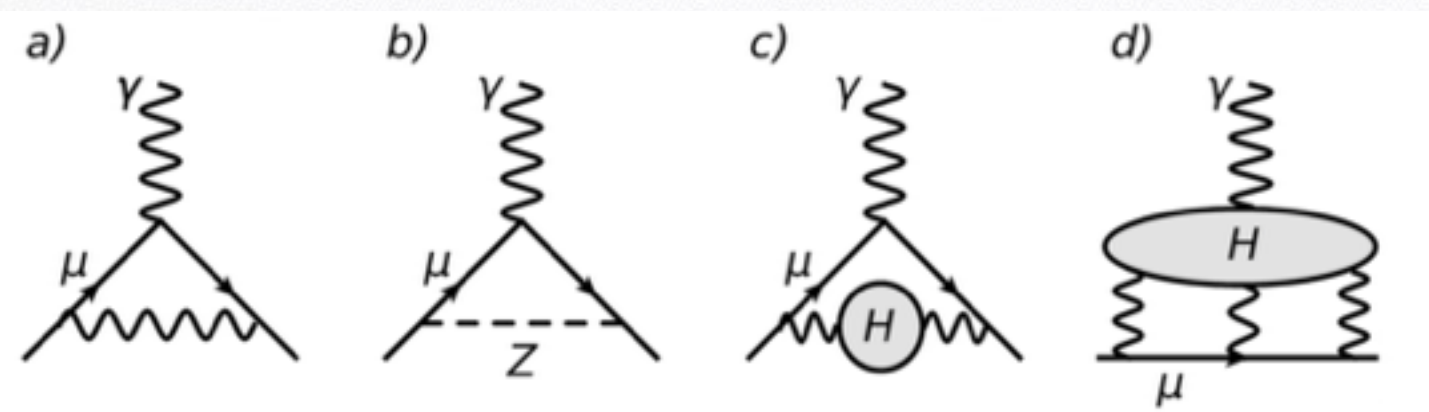

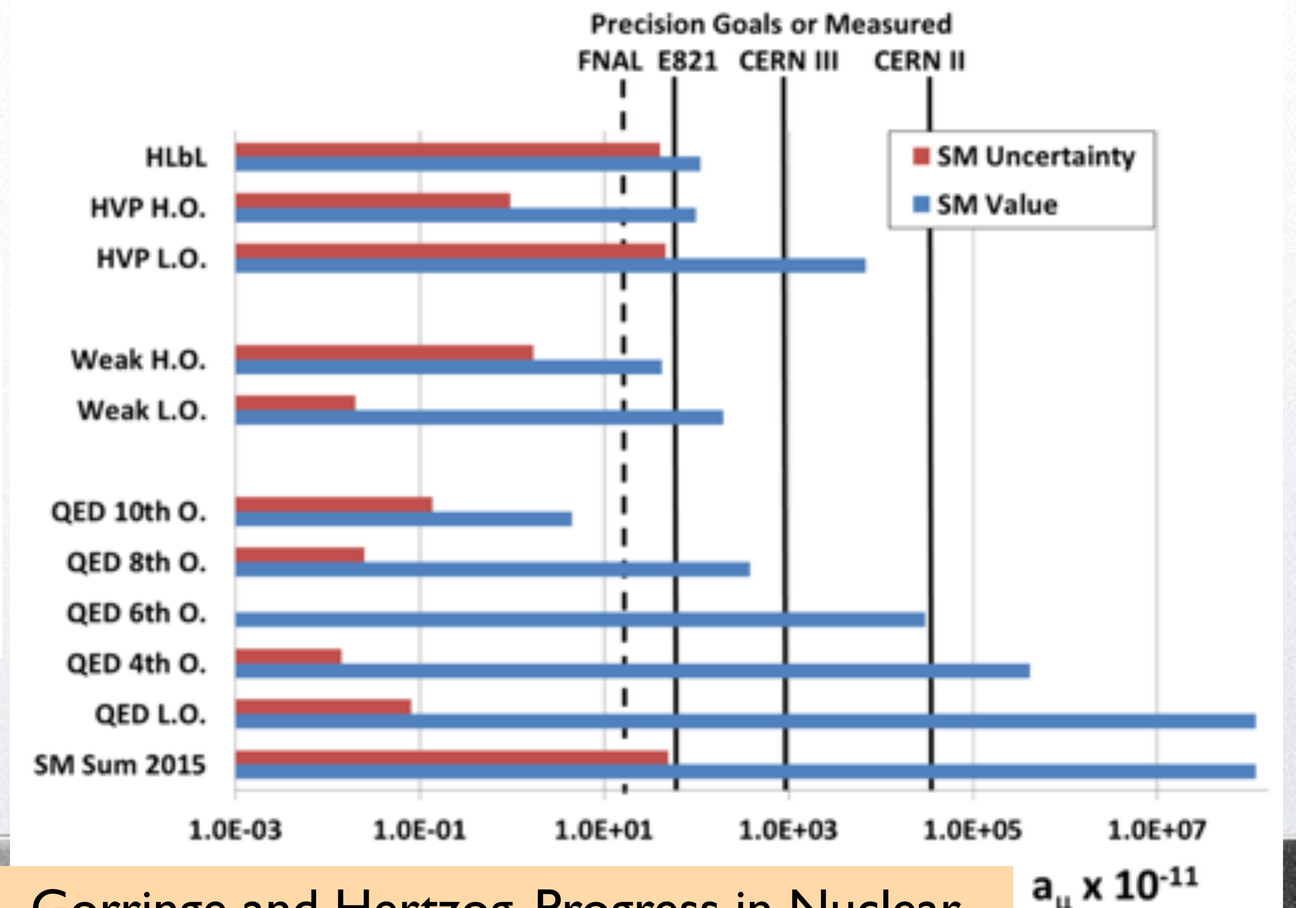

Gorringe and Hertzog, Progress in Nuclear and Particle Physics, *to appear*

Current Experimental Status for a_μ

- Current best measurement from E-821 at Brookhaven

$$a_\mu(\mathrm{SM}_a) = 1\ 165\ 918\ 02(49) \times 10^{-11}\ (0.42\mathrm{ppm})$$ EPJ-C **71**, 1515 (2011)

$$a_\mu(\mathrm{SM}_b) = 1\ 165\ 918\ 28(50) \times 10^{-11}\ (0.43\mathrm{ppm})$$ J. Phys G **38**, 085003 (2011)

$$a_\mu(\mathrm{exp}) = 1\ 165\ 920\ 89(63) \times 10^{-11}\ (0.54\mathrm{ppm})$$ Phys. Rev. D **73**, 072003 (2008)

- >3σ disagreement between theory and experiment

$$\Delta a_\mu(\mathrm{exp} - \mathrm{SM}_a) = 287(80) \times 10^{-11}\ (3.6\sigma)$$
$$\Delta a_\mu(\mathrm{exp} - \mathrm{SM}_b) = 261(80) \times 10^{-11}\ (3.3\sigma)$$

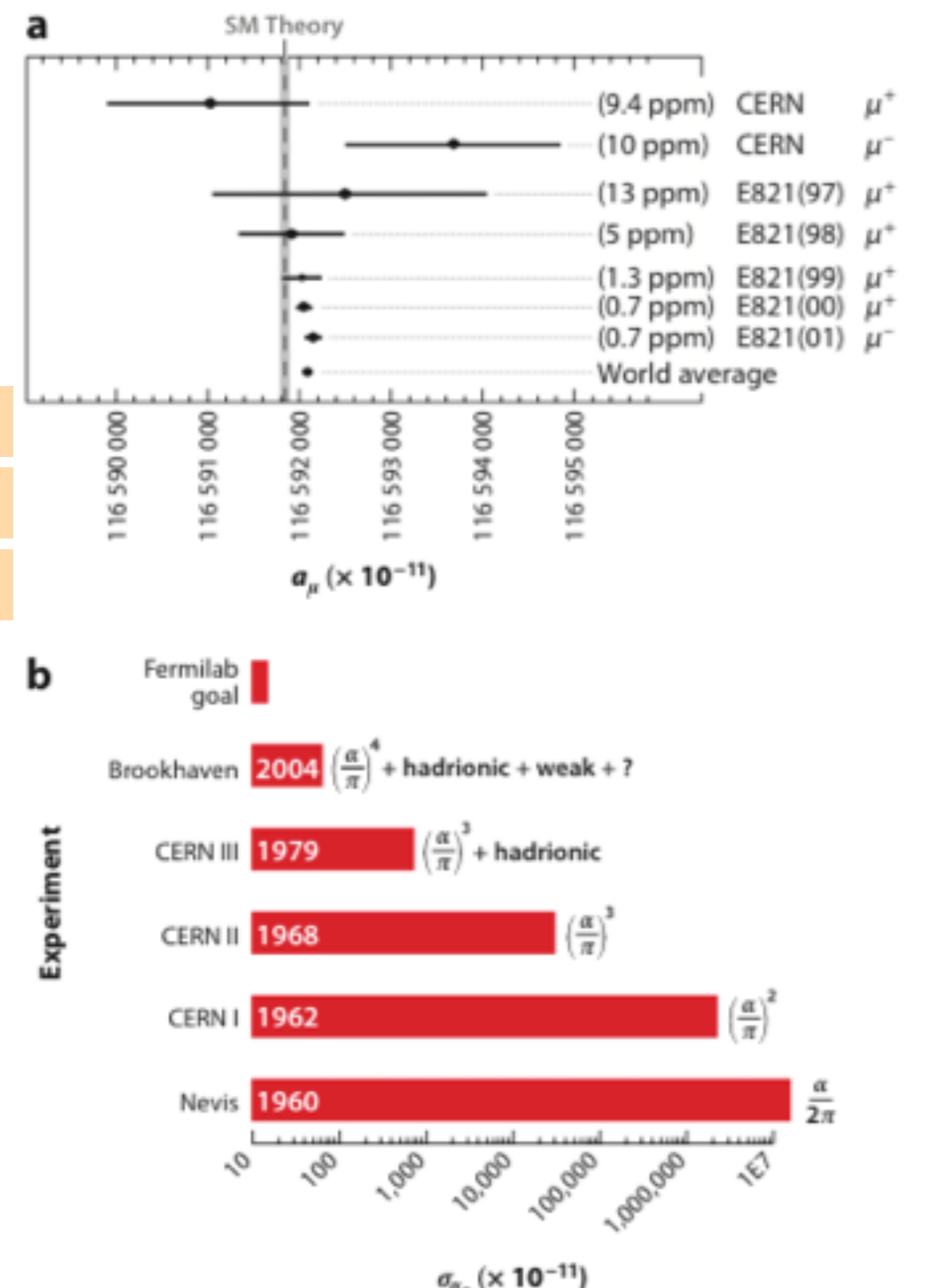

Annu. Rev. Nucl. Part. Sci. **62**, 237 (2012)

Measuring a_μ

The Key Point

- Ultimately, the magnetic moment a measure of how strongly the particle interacts with a magnetic field
- If we assume the particle spin is 1/2, then it boils down to
  - Having a well-measured magnetic field
  - Passing a particle through that field and measuring some effect

Storage Ring Experiments

- Muons produced from pion decays. V-A nature of weak decay results in polarized muons
- In a storage ring,
  - Muons circulate at cyclotron frequency
  - Spin precesses at Larmor frequency
  - Difference gives direct measure of a_μ
- When muon decays, higher energy positrons preferentially emitted in direction of muon spin
  - Selecting high energy decay positrons "imprints" ω_a frequency onto the decay spectrum

Storage Ring Experiments

- Muons produced from pion decays. V-A nature of weak decay results in polarized muons
- In a storage ring,
  - Muons circulate at cyclotron frequency

$$\omega_c = \frac{eB}{mc}$$

  - Spin precesses at Larmor frequency
  - Difference gives direct measure of a_μ
- When muon decays, higher energy positrons preferentially emitted in direction of muon spin
  - Selecting high energy decay positrons "imprints" ω_a frequency onto the decay spectrum

Storage Ring Experiments

- Muons produced from pion decays. V-A nature of weak decay results in polarized muons
- In a storage ring,
  - Muons circulate at cyclotron frequency
  - Spin precesses at Larmor frequency
  - Difference gives direct measure of a_μ
- When muon decays, higher energy positrons preferentially emitted in direction of muon spin
  - Selecting high energy decay positrons "imprints" ω_a frequency onto the decay spectrum

$$\omega_c = \frac{eB}{mc}$$

$$\omega_s = g\frac{eB}{2mc}$$

Storage Ring Experiments

- Muons produced from pion decays. V-A nature of weak decay results in polarized muons
- In a storage ring,
  - Muons circulate at cyclotron frequency
  - Spin precesses at Larmor frequency
  - Difference gives direct measure of a_μ
- When muon decays, higher energy positrons preferentially emitted in direction of muon spin
  - Selecting high energy decay positrons "imprints" ω_a frequency onto the decay spectrum

$$\omega_c = \frac{eB}{mc}$$

$$\omega_s = g\frac{eB}{2mc}$$

$$\omega_a = \omega_s - \omega_c$$

$$\omega_a = a_\mu \frac{eB}{mc}$$

E821 “Wiggle” Plot

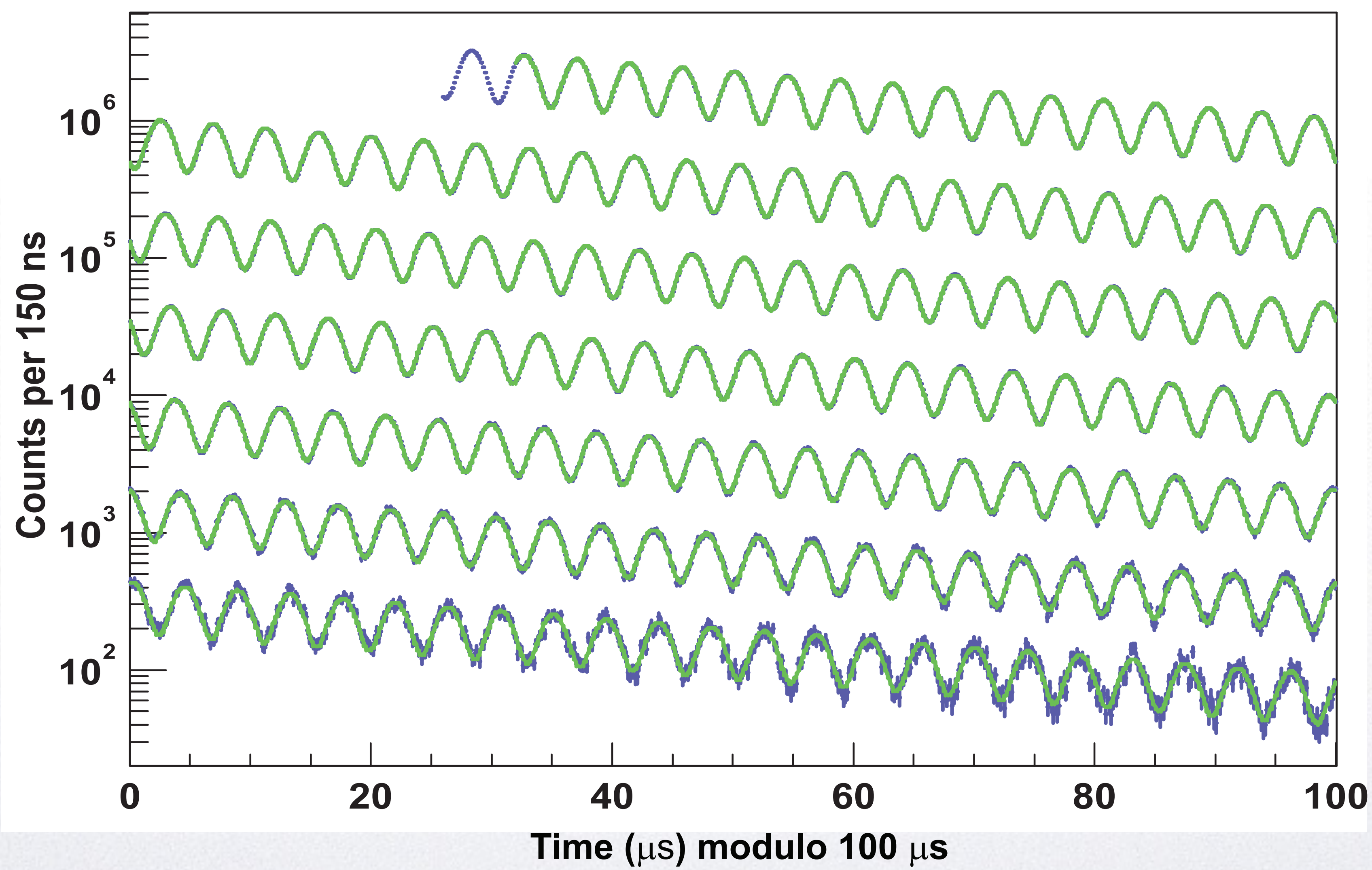

Phys. Rev. D **73**, 072003 (2008)

E-989 at Fermilab

http://muon-g-2.fnal.gov

The Magic Momentum

- Muons bent into a circle with a magnetic field in the storage ring
- But, beam focusing is also need. Done with electrostatic quadrupoles.
- In the presence of electric and magnetic fields,

$$\vec{\omega}_a = \frac{e}{mc}\left[a\vec{B} - \left(a - \frac{1}{\gamma^2 - 1}\right)\vec{\beta} \times \vec{E}\right]$$

- Choosing γ=29.3 (p=3.09 GeV) cancels out E-field term!

The Magic Momentum

- Muons bent into a circle with a magnetic field in the storage ring
- But, beam focusing is also need. Done with electrostatic quadrupoles.
- In the presence of electric and magnetic fields,

$$\vec{\omega}_a = \frac{e}{mc}\left[a\vec{B} - \cancel{\left(a - \frac{1}{\gamma^2 - 1}\right)\vec{\beta} \times \vec{E}}\right]$$

- Choosing γ=29.3 (*p*=3.09 GeV) cancels out E-field term!

Why Fermilab?

- Fermilab is able to produce many more muons, than Brookhaven
- Fermilab is able to produce “better” muons than Brookhaven
  - Much less pion contamination makes it into the ring
- Improve a_μ measurement to 0.14 ppm
  - Assuming central values unchanged, will result in 5σ experimental/theoretical discrepancy

Experiment Overview

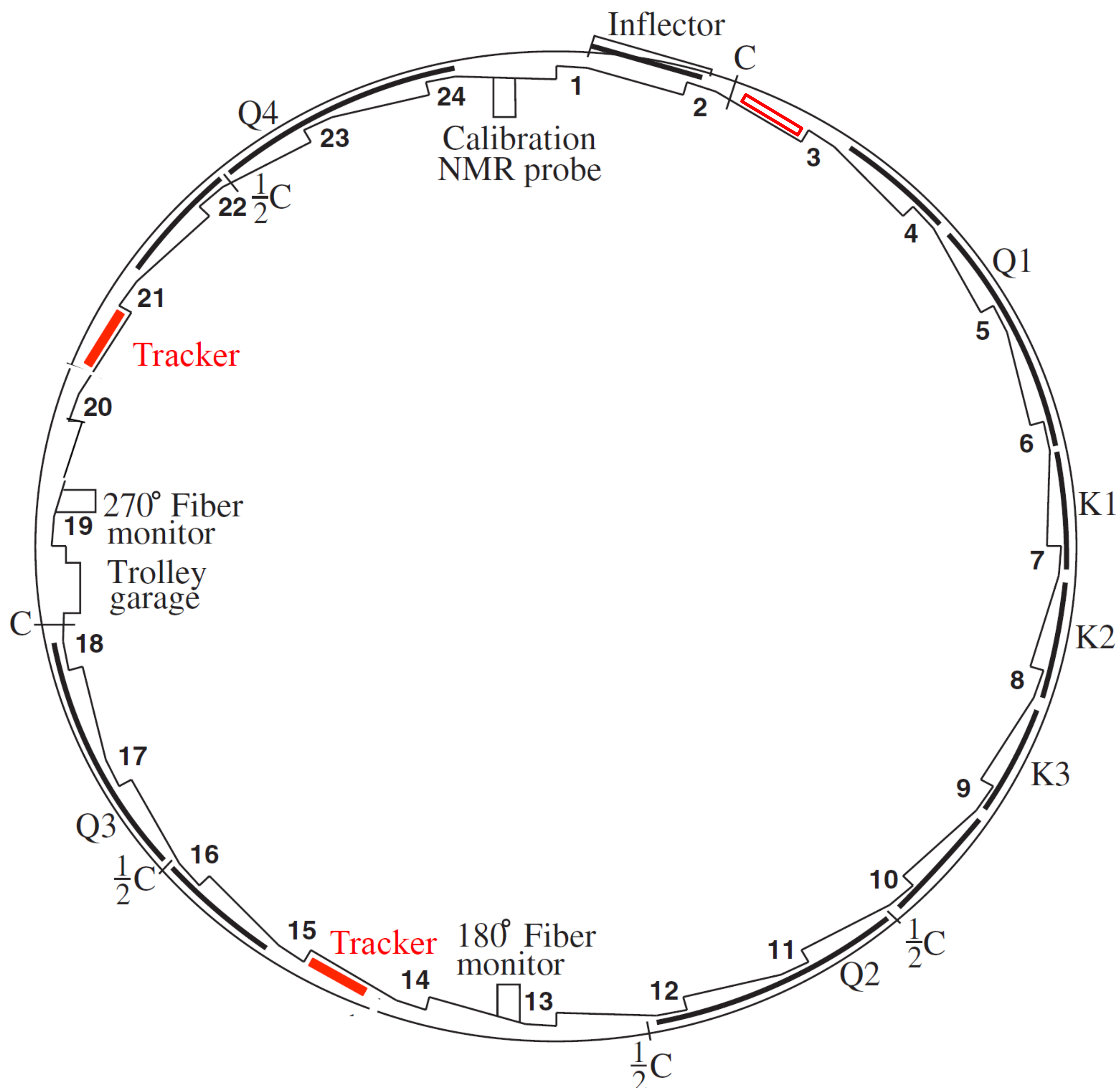

- 1.4T, 14m-diameter superconducting storage magnet
- 24 calorimeter stations
- 3 straw tube tracker stations
- 2 fiber harps
- Entrance counter
- Beam position monitors

The Collaboration

J. Grange, P. Winter
Argonne National Laboratory

R.M. Carey, E. Hazen, N. Kinnaird, J.P. Miller, J. Mott, B.L. Roberts*
Boston University

J. Crnkovic, W.M. Morse, H. Kamal Sayed, V. Tishchenko
Brookhaven National Laboratory

V.P. Druzhinin, I.A. Koop, I. Logashenko[1], Y.M. Shatunov, E. Solodov
Budker Institute of Nuclear Physics

R. Bjorkquist, A. Chapelain, N. Eggert, A. Frankenthal, L. Gibbons, S. Kim, A. Mikhailichenko, Y. Orlov, N. Rider, D. Rubin, D. Sweigart
Cornell University

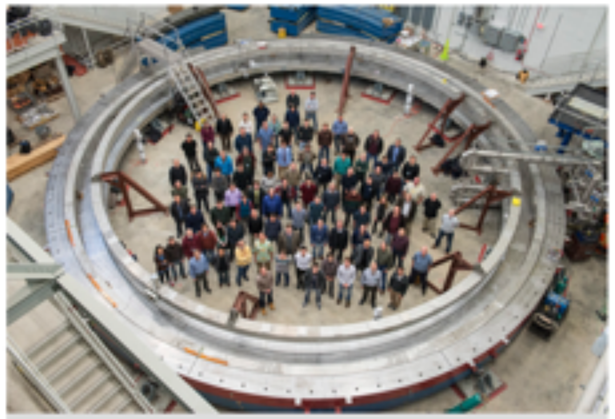

The Muon g-2 collaboration

D. Allspach, E. Barzi, B. Casey, M.E. Convery, B. Drendel, H. Freidsam, C. Johnstone, J. Johnstone, B. Kiburg, I. Kourbanis, A.L. Lyon, K.W. Merritt, J.P. Morgan, H. Nguyen, J-F. Ostiguy, A. Para, C.C. Polly**, M. Popovic, E. Ramberg, M. Rominsky, A.K. Soha, D. Still, T. Walton, C. Yoshikawa
Fermi National Accelerator Laboratory

K. Jungmann, C.J.G. Onderwater
University of Groningen, KVI

P. Debevec, S. Leo, K. Pitts, C. Schlesier
University of Illinois at Urbana-Champaign

S. Catalonotti[2], R. D. Stefano[3], M. Iacovacci[2], S. Marignetti[3], S. Mastroianni, G. D. Sciascio, D. Moricciani, G. Cantatore[4], M. Karuza[5]
Istituto Nazionale di Fisica Nucleare - Sezione di Napoli

K. Giovanetti
James Madison University

V. Baranov, V. Duginov, N. Khomutov, V. Krylov, N. Kuchinskiy, V. Volnykh
Joint Institute for Nuclear Research, Dubna

M. Gaisser[6], S. Haciomeroglu[6], Y. Kim[6], S. Lee[6], M. Lee[6], Y. K. Semertzidis[6], E. Won[7]
KAIST

R. Fatemi, W. Gohn, T. Gorringe
University of Kentucky

A. Anastasi[8], D. Babusci, R. Cimino, G. Corradi, S. Dabagov[9], C. Ferrari[10], A. Fioretti[10], C. Gabbanini[10], D. Hampai, A. Palladino, G. Venanzoni
Laboratori Nazionali di Frascati

T. Bowcock, J. Carroll, B. King, S. Maxfield, A. Smith, T. Teubner, M. Whitley, A. Wolski[11], M. Wormald
University of Liverpool

S. Al-Kilani, R. Chislett, M. Lancaster, E. Motuk, T. Stuttard, M. Warren
University of College London

D. Flay, D. Kawall, Z. Meadows
University of Massachusetts

M. Syphers[12], D. Tarazona[12]
Michigan State University

T. Chupp, A. Tewlsey-Booth
University of Michigan

B. Quinn
University of Mississippi

M. Eads, A. Epps, G. Luo, M. McEvoy, N. Pohlman, M. Shenk
Northern Illinois University

A. de Gouvea, H. Schellman[13], L. Welty-Rieger
Northwestern University

B. Abi, F. Azfar, S. Henry,
University of Oxford

F. Gray
Regis University

C. Fu[14], X. Ji[14], L. Li[14], H. Yang[14]
Shanghai Jiao Tong University

D. Stockinger
Technische Universitat Dresden

D. Cauz[15], G. Pauletta[15], L. Santi[15]
Universitá Udine

S. Baessler[16], E. Frlez, D. Pocanic
University of Virginia

L. P. Alonzi, M. Fertl, A. Fienberg, N. Froemming, A. Garcia, D. W. Hertzog*, P. Kammel, J. Kaspar, R. Osofsky, M. Smith, E. Swanson
University of Washington

K. Lynch
York College, CUNY

~100 physicists
~30 institutions
8 countries

The Plan

From E-989 Technical Design Report

Table 5.3: The largest systematic uncertainties for the final E821 ω_a analysis and proposed upgrade actions and projected future uncertainties for data analyzed using the T method. The relevant Chapters and Sections are given where specific topics are discussed in detail.

Category	E821 [ppm]	E989 Improvement Plans	Goal [ppm]	Chapter & Section
Gain changes	0.12	Better laser calibration		
		low-energy threshold	0.02	17.3.1
Pileup	0.08	Low-energy samples recorded		
		calorimeter segmentation	0.04	17.3.2
Lost muons	0.09	Better collimation in ring	0.02	14.4
CBO	0.07	Higher n value (frequency)		
		Better match of beamline to ring	< 0.03	14.3.1
E and pitch	0.05	Improved tracker		
		Precise storage ring simulations	0.03	14.3.2
Total	0.18	Quadrature sum	0.07	

arXiv: 1501.06858

Note: Statistical uncertainty not included in these tables

Table 5.4: Systematic uncertainties estimated for the magnetic field, ω_p, measurement. The final E821 values are given for reference, and the proposed upgrade actions are projected. Note, several items involve ongoing R&D, while others have dependencies on the uniformity of the final shimmed field, which cannot be known accurately at this time. The relevant Chapters and Sections are given where specific topics are discussed in detail.

Category	E821 [ppm]	Main E989 Improvement Plans	Goal [ppm]	Chapter
Absolute field calibration	0.05	Special 1.45 T calibration magnet with thermal enclosure; additional probes; better electronics	0.035	16.4.1
Trolley probe calibrations	0.09	Plunging probes that can cross calibrate off-central probes; better position accuracy by physical stops and/or optical survey; more frequent calibrations	0.03	16.4.1
Trolley measurements of B_0	0.05	Reduced position uncertainty by factor of 2; improved rail irregularities; stabilized magnet field during measurements*	0.03	16.3.1
Fixed probe interpolation	0.07	Better temperature stability of the magnet; more frequent trolley runs	0.03	16.3
Muon distribution	0.03	Additional probes at larger radii; improved field uniformity; improved muon tracking	0.01	16.3
Time-dependent external magnetic fields	–	Direct measurement of external fields; simulations of impact; active feedback	0.005	16.6
Others †	0.10	Improved trolley power supply; trolley probes extended to larger radii; reduced temperature effects on trolley; measure kicker field transients	0.03	16.7
Total systematic error on ω_p	0.17		0.07	16

*Improvements in many of these categories will also follow from a more uniformly shimmed main magnetic field.

†Collective smaller effects in E821 from higher multipoles, trolley temperature uncertainty and its power supply voltage response, and eddy currents from the kicker. See 16.7.

The Plan

From E-989 Technical Design Report

Table 5.3: The largest systematic uncertainties for the final E821 ω_a analysis and proposed upgrade actions and projected future uncertainties for data analyzed using the T method. The relevant Chapters and Sections are given where specific topics are discussed in detail.

Detector Improvements

Category	E821 [ppm]	E989 Improvement Plans	Goal [ppm]	Chapter & Section
Gain changes	0.12	Better laser calibration low-energy threshold	0.02	17.3.1
Pileup	0.08	Low-energy samples recorded calorimeter segmentation	0.04	17.3.2
Lost muons	0.09	Better collimation in ring	0.02	14.4
CBO	0.07	Higher n value (frequency) Better match of beamline to ring	< 0.03	14.3.1
E and pitch	0.05	Improved tracker Precise storage ring simulations	0.03	14.3.2
Total	0.18	Quadrature sum	0.07	

arXiv: 1501.06858

Note: Statistical uncertainty not included in these tables

Table 5.4: Systematic uncertainties estimated for the magnetic field, ω_p, measurement. The final E821 values are given for reference, and the proposed upgrade actions are projected. Note, several items involve ongoing R&D, while others have dependencies on the uniformity of the final shimmed field, which cannot be known accurately at this time. The relevant Chapters and Sections are given where specific topics are discussed in detail.

Category	E821 [ppm]	Main E989 Improvement Plans	Goal [ppm]	Chapter
Absolute field calibration	0.05	Special 1.45 T calibration magnet with thermal enclosure; additional probes; better electronics	0.035	16.4.1
Trolley probe calibrations	0.09	Plunging probes that can cross calibrate off-central probes; better position accuracy by physical stops and/or optical survey; more frequent calibrations	0.03	16.4.1
Trolley measurements of B_0	0.05	Reduced position uncertainty by factor of 2; improved rail irregularities; stabilized magnet field during measurements*	0.03	16.3.1
Fixed probe interpolation	0.07	Better temperature stability of the magnet; more frequent trolley runs	0.03	16.3
Muon distribution	0.03	Additional probes at larger radii; improved field uniformity; improved muon tracking	0.01	16.3
Time-dependent external magnetic fields	–	Direct measurement of external fields; simulations of impact; active feedback	0.005	16.6
Others †	0.10	Improved trolley power supply; trolley probes extended to larger radii; reduced temperature effects on trolley; measure kicker field transients	0.03	16.7
Total systematic error on ω_p	0.17		0.07	16

*Improvements in many of these categories will also follow from a more uniformly shimmed main magnetic field.

†Collective smaller effects in E821 from higher multipoles, trolley temperature uncertainty and its power supply voltage response, and eddy currents from the kicker. See 16.7.

The Plan

From E-989 Technical Design Report

Table 5.3: The largest systematic uncertainties for the final E821 ω_a analysis and proposed upgrade actions and projected future uncertainties for data analyzed using the T method. The relevant Chapters and Sections are given where specific topics are discussed in detail.

Category	E821 [ppm]	E989 Improvement Plans	Goal [ppm]	Chapter & Section
Gain changes	0.12	Better laser calibration low-energy threshold	0.02	17.3.1
Pileup	0.08	Low-energy samples recorded calorimeter segmentation	0.04	17.3.2
Lost muons	0.09	Better collimation in ring	0.02	14.4
CBO	0.07	Higher n value (frequency) Better match of beamline to ring	< 0.03	14.3.1
E and pitch	0.05	Improved tracker Precise storage ring simulations	0.03	14.3.2
Total	0.18	Quadrature sum	0.07	

Detector Improvements

arXiv: 1501.06858

Note: Statistical uncertainty not included in these tables

Table 5.4: Systematic uncertainties estimated for the magnetic field, ω_p, measurement. The final E821 values are given for reference, and the proposed upgrade actions are projected. Note, several items involve ongoing R&D, while others have dependencies on the uniformity of the final shimmed field, which cannot be known accurately at this time. The relevant Chapters and Sections are given where specific topics are discussed in detail.

Category	E821 [ppm]	Main E989 Improvement Plans	Goal [ppm]	Chapter
Absolute field calibration	0.05	Special 1.45 T calibration magnet with thermal enclosure; additional probes; better electronics	0.035	16.4.1
Trolley probe calibrations	0.09	Plunging probes that can cross calibrate off-central probes; better position accuracy by physical stops and/or optical survey; more frequent calibrations	0.03	16.4.1
Trolley measurements of B_0	0.05	Reduced position uncertainty by factor of 2; improved rail irregularities; stabilized magnet field during measurements*	0.03	16.3.1
Fixed probe interpolation	0.07	Better temperature stability of the magnet; more frequent trolley runs	0.03	16.3
Muon distribution	0.03	Additional probes at larger radii; improved field uniformity; improved muon tracking	0.01	16.3
Time-dependent external magnetic fields	–	Direct measurement of external fields; simulations of impact; active feedback	0.005	16.6
Others †	0.10	Improved trolley power supply; trolley probes extended to larger radii; reduced temperature effects on trolley; measure kicker field transients	0.03	16.7
Total systematic error on ω_p	0.17		0.07	16

*Improvements in many of these categories will also follow from a more uniformly shimmed main magnetic field.
†Collective smaller effects in E821 from higher multipoles, trolley temperature uncertainty and its power supply voltage response, and eddy currents from the kicker. See 16.7.

Magnetic Field Improvements

Fermilab Muon Campus

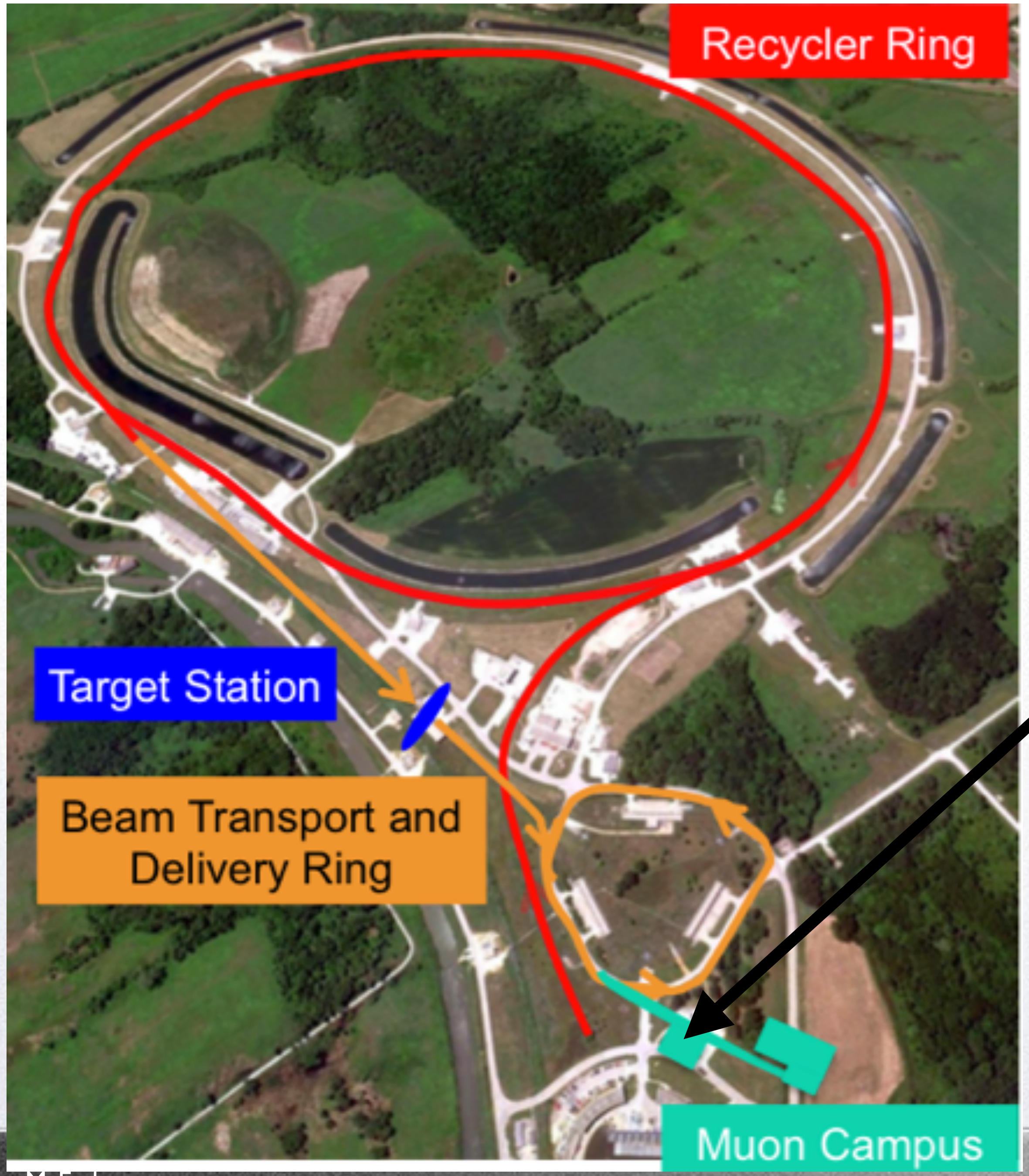

- A new campus at Fermilab is being constructed to host the next generation of muon experiments
- The new *g*-2 experiment will be housed in the MC-1 building
- Construction on mu2e building and beam line recently started

Ring Reassembly

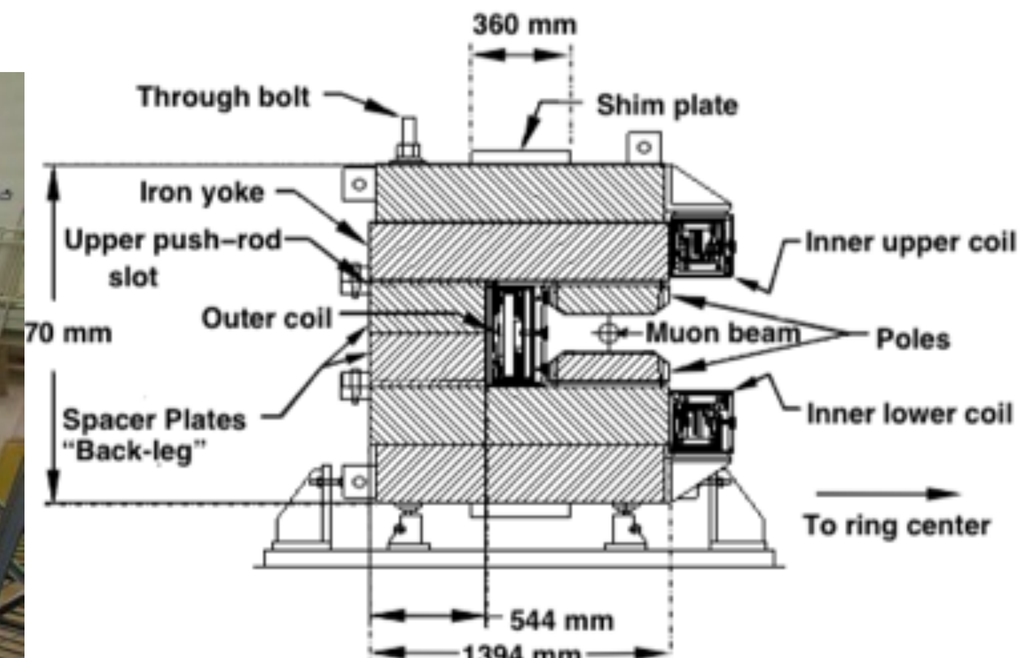

Ring in the process of being cooled and powered

Next comes 6-9 months of mechanical shimming to get uniformity to a few ppm

Measuring the Magnetic Field

- One plunging NMR probe for absolute calibration
- 375 fixed NMR probes outside storage region
- 17 NMR probes on trolley that moves around storage region
- All NMR probes being reworked

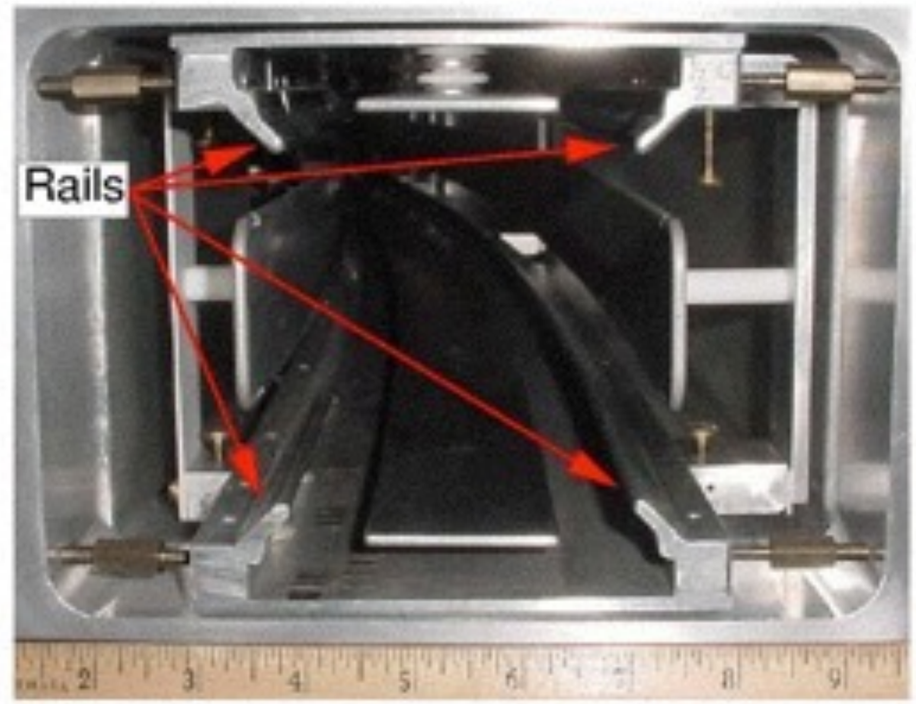

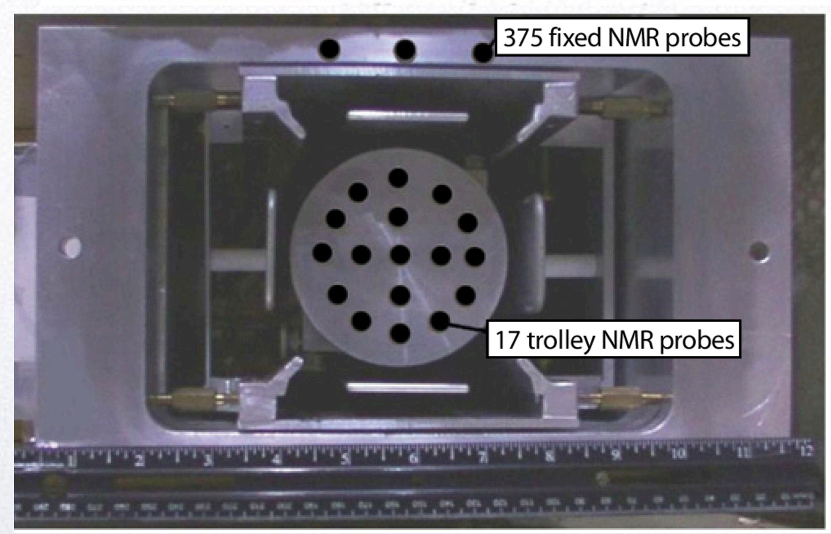

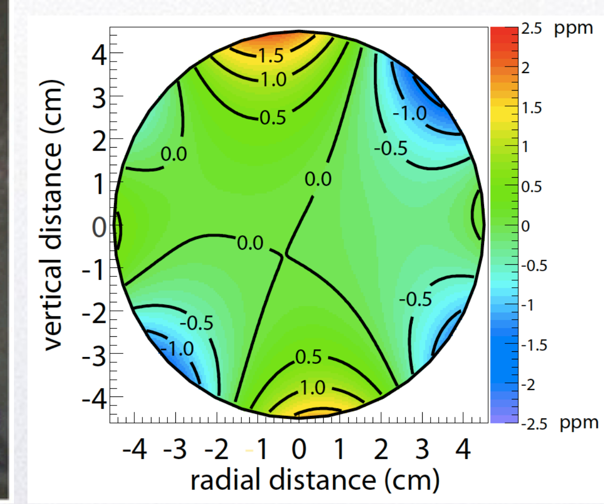

Calorimeters

- 24 calorimeter stations around ring to detect decay positrons
- 9x5 array of PbF_2 crystals read out by SiPM
- Finalizing design, including extensive testbeam efforts
- Associated laser calibration system to monitor gain
- Recent results show energy resolution of 3-5%/$\sqrt{E}$ and time stability better than 0.1%

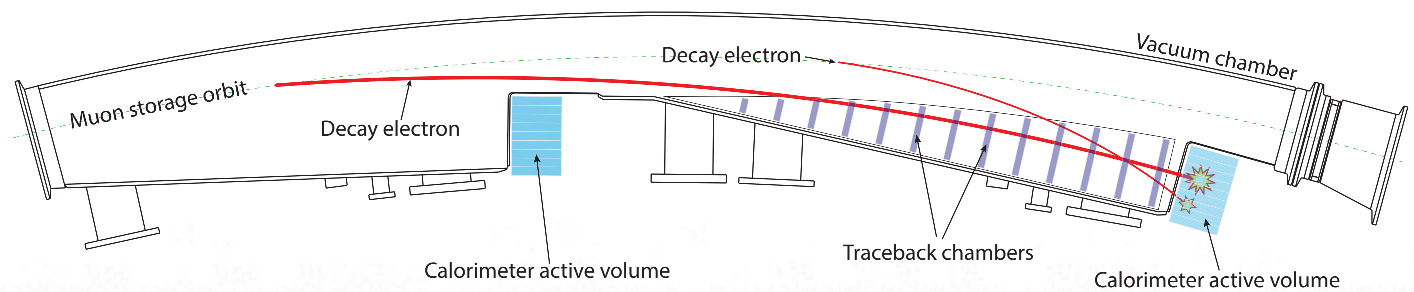

arXiv: 1412.5525
arXiv: 1504.00132

Calorimeters

- 24 calorimeter stations around ring to detect decay positrons
- 9x5 array of PbF_2 crystals read out by SiPM
- Finalizing design, including extensive testbeam efforts
- Associated laser calibration system to monitor gain
- Recent results show energy resolution of 3-5%/$\sqrt{E}$ and time stability better than 0.1%

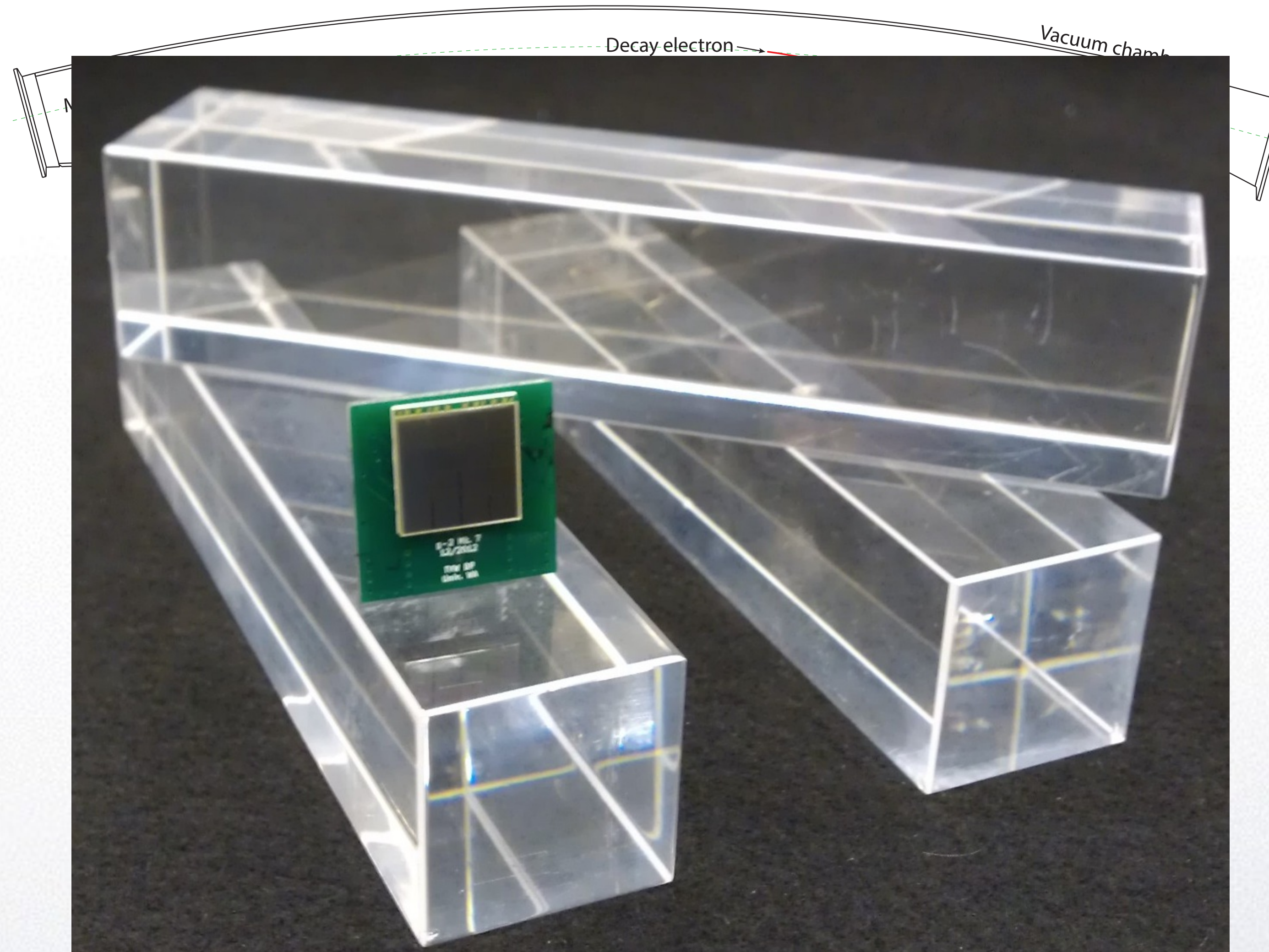

arXiv: 1412.5525
arXiv: 1504.00132

Calorimeters

- 24 calorimeter stations around ring to detect decay positrons
- 9x5 array of PbF_2 crystals read out by SiPM
- Finalizing design, including extensive testbeam efforts
- Associated laser calibration system to monitor gain
- Recent results show energy resolution of 3-5%/$\sqrt{E}$ and time stability better than 0.1%

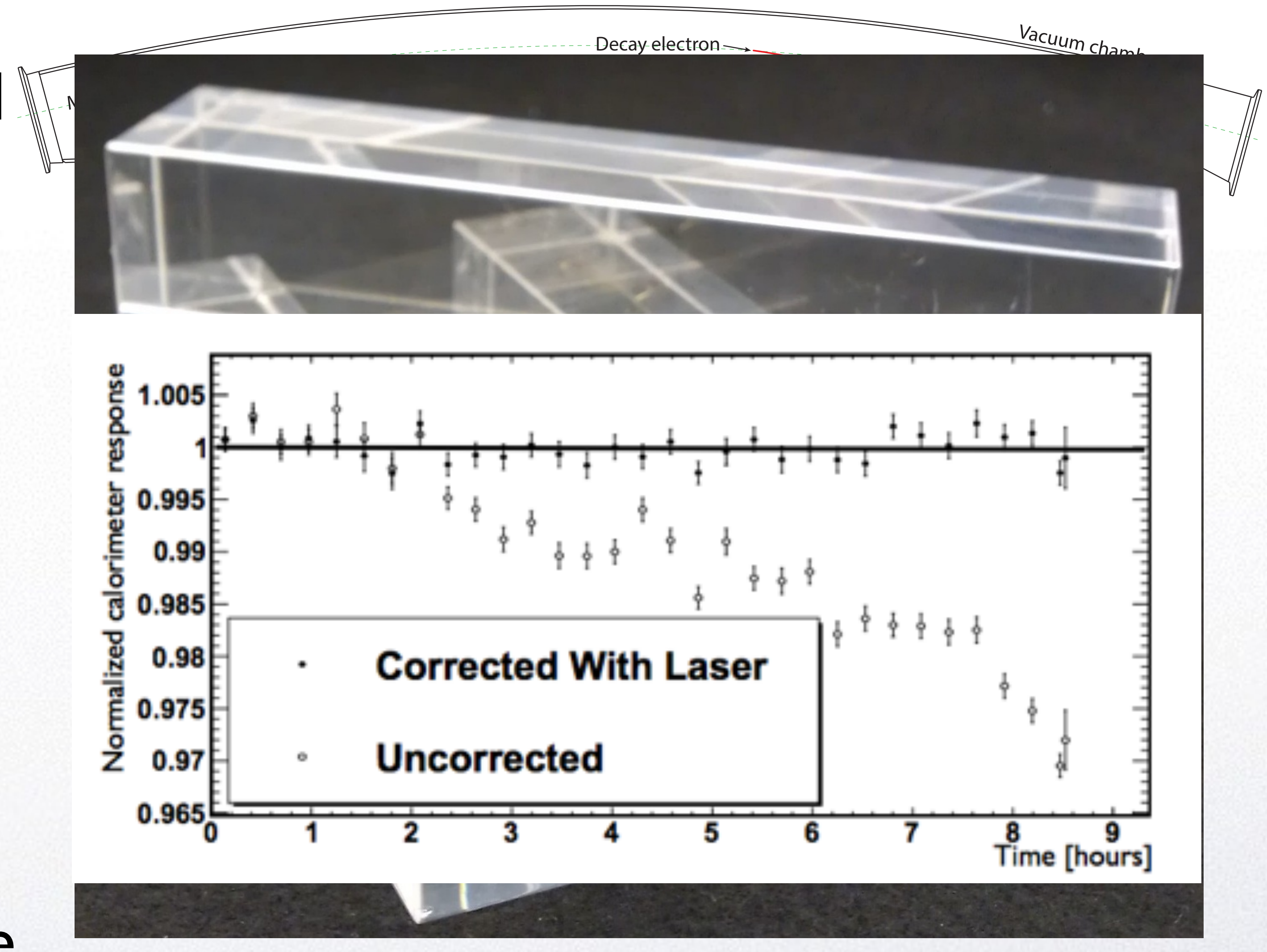

arXiv: 1412.5525
arXiv: 1504.00132

Auxiliary Detectors

- Fiber harps: Scintillating fibers on a frame which can be rotated into storage region for a (destructive) measurement of beam parameters
- T0 counter - thin plastic at entrance to storage ring (attached to photodetector) to measure time muons enter the ring
- Beam position monitors - three planes of scintillating fibers to measure muon beam profile at entrance to storage ring

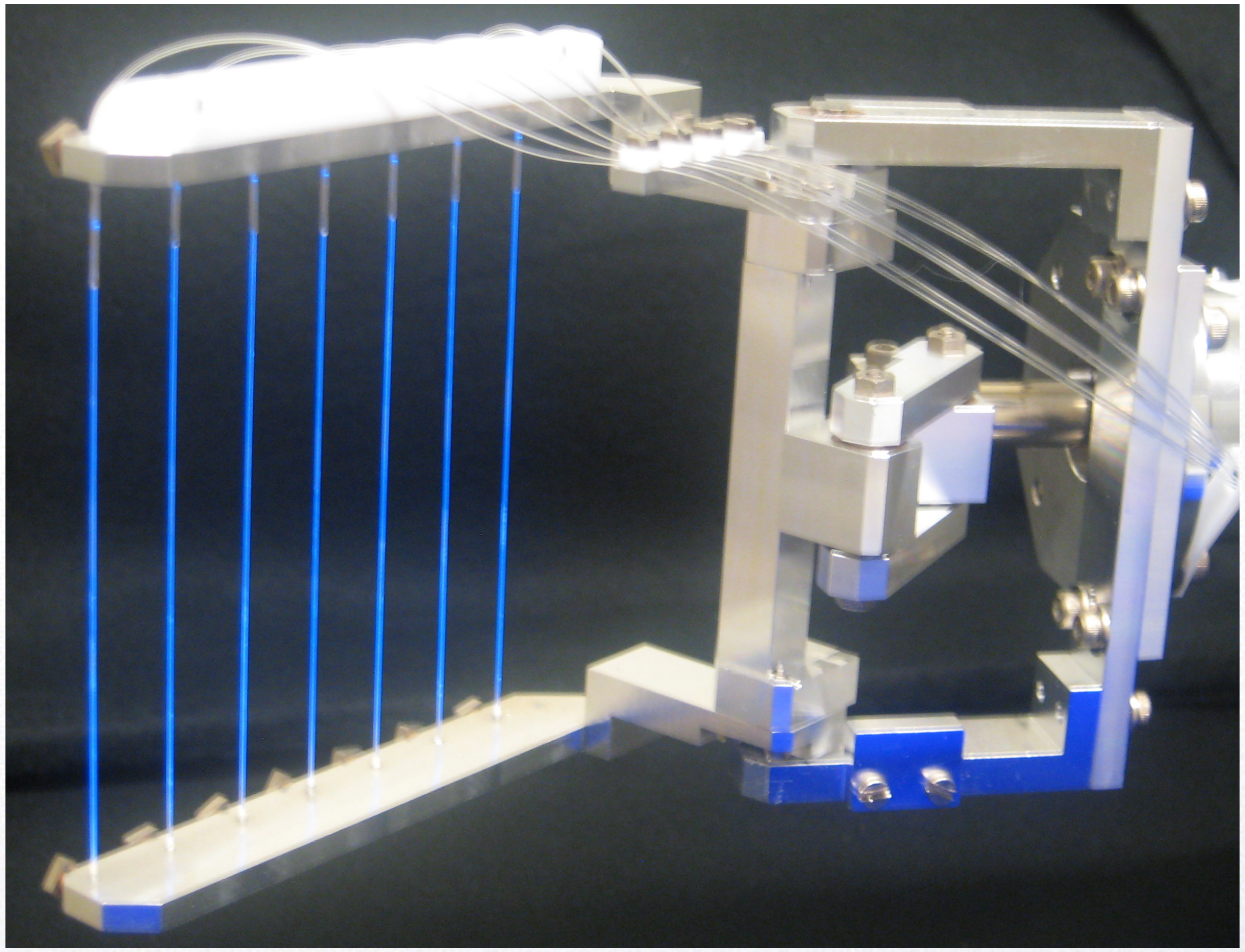

Auxiliary Detectors

- Fiber harps: Scintillating fibers on a frame which can be rotated into storage region for a (destructive) measurement of beam parameters
- T0 counter - thin plastic at entrance to storage ring (attached to photodetector) to measure time muons enter the ring
- Beam position monitors - three planes of scintillating fibers to measure muon beam profile at entrance to storage ring

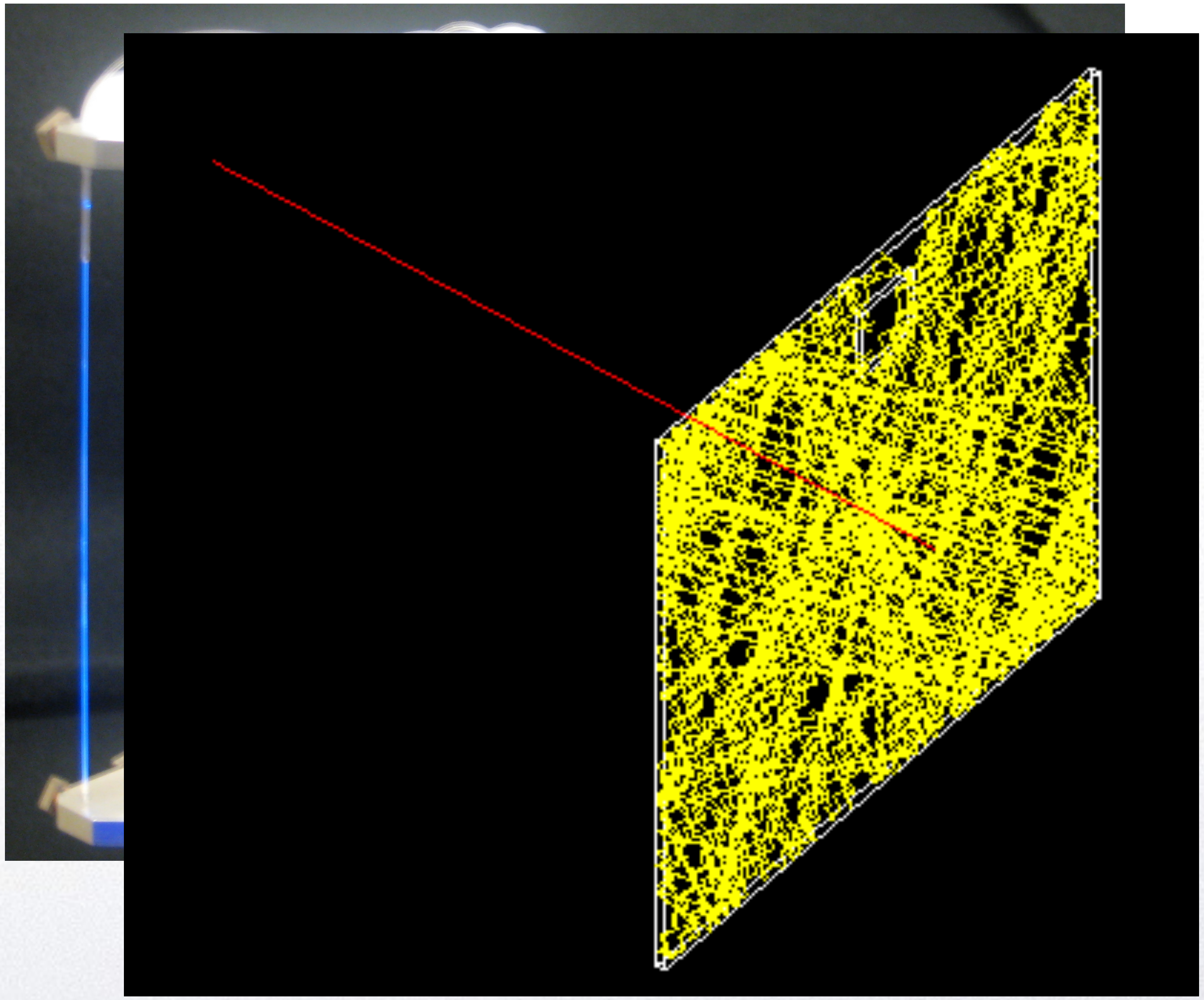

Auxiliary Detectors

- Fiber harps: Scintillating fibers on a frame which can be rotated into storage region for a (destructive) measurement of beam parameters
- T0 counter - thin plastic at entrance to storage ring (attached to photodetector) to measure time muons enter the ring
- Beam position monitors - three planes of scintillating fibers to measure muon beam profile at entrance to storage ring

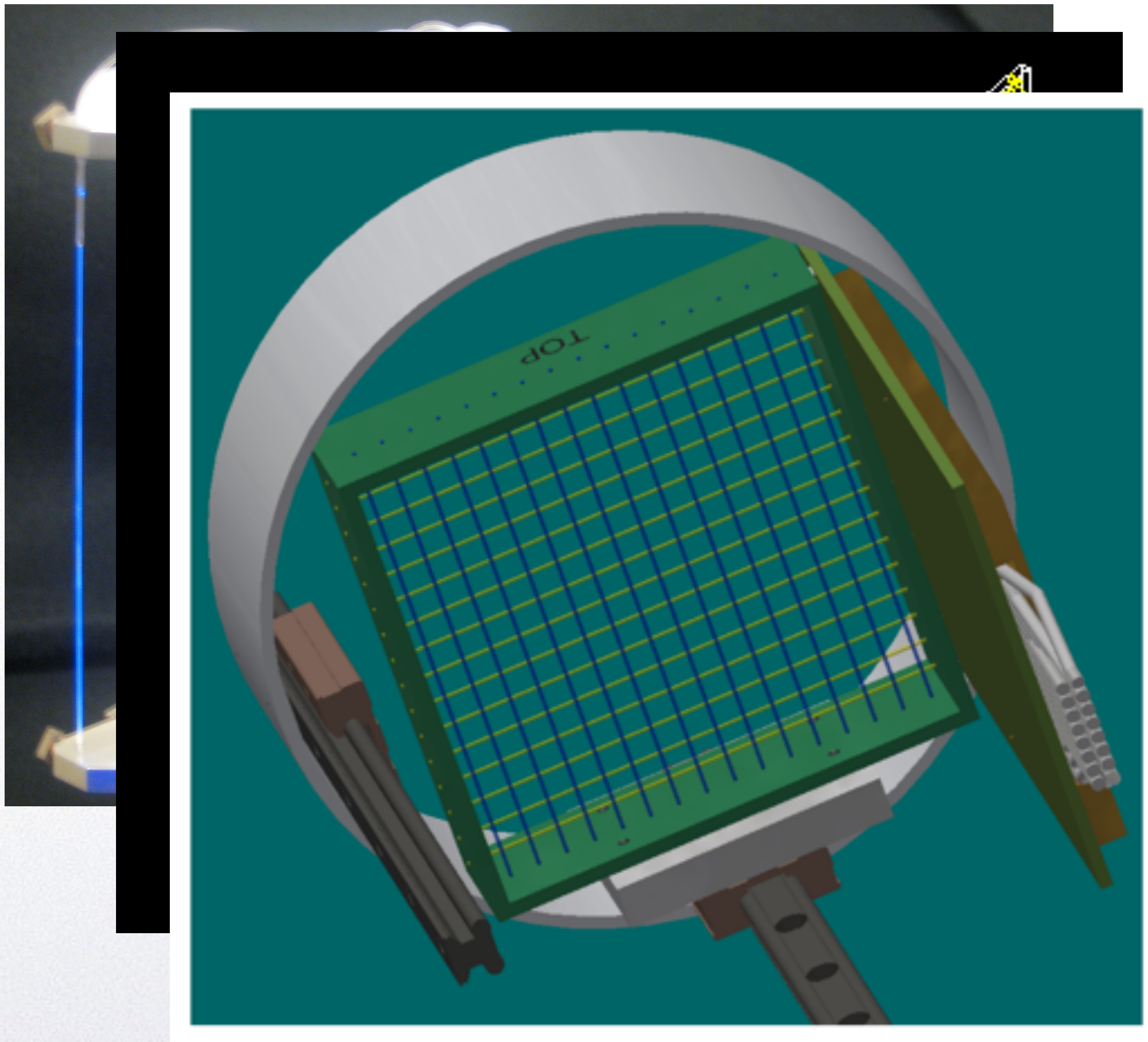

Straw Tube Trackers

- Three tracker stations around the ring
- Each station has 8 tracking modules in the scalloped region in front of a calorimeter
- Each module has ~200 aluminized mylar straws with 15μm walls, 5mm in diameter, 12cm long. Wire is 50um at 1.8kV, 50:50 Ar:Ethane gas at 1atm

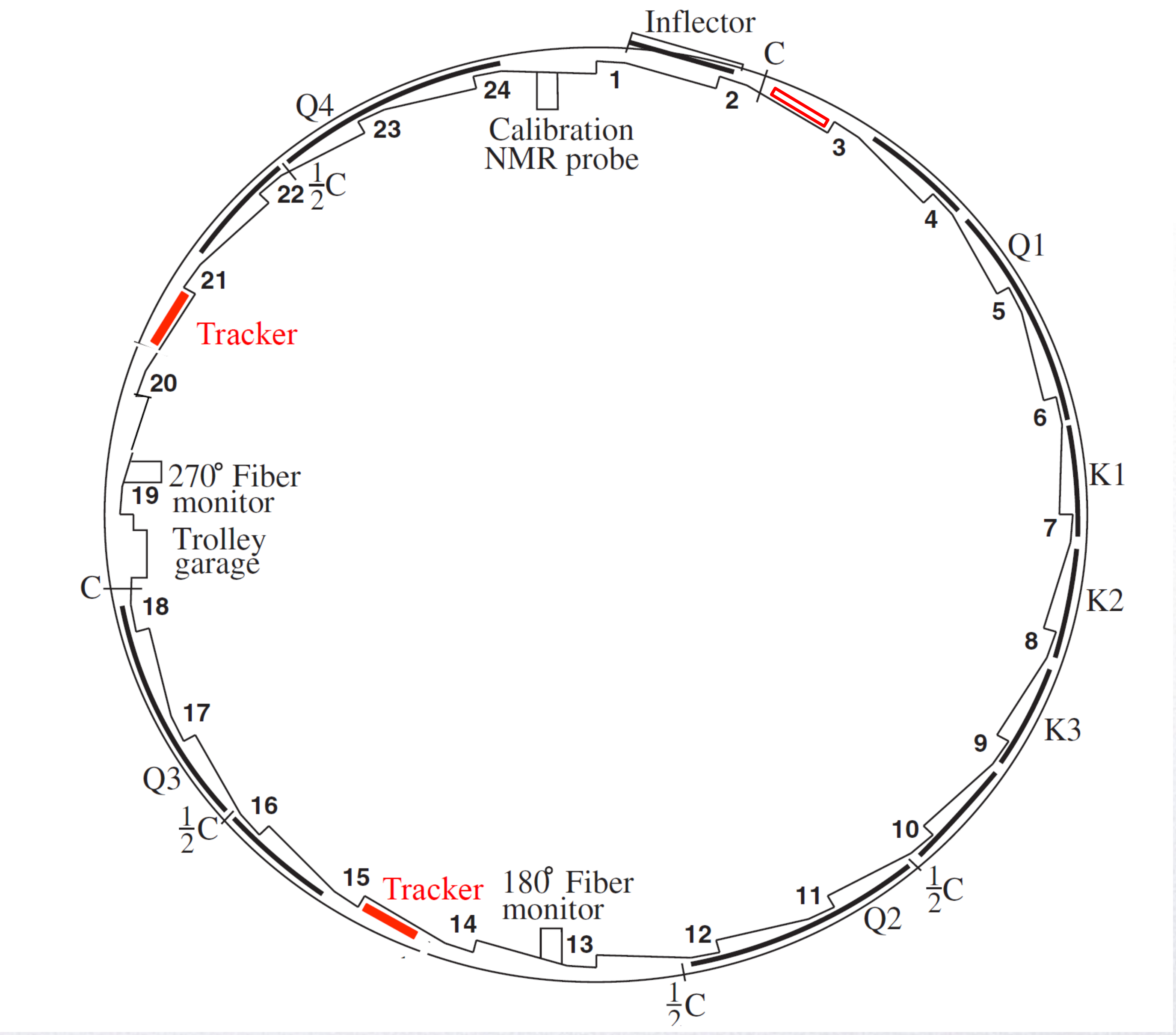

Straw Tube Trackers

- Three tracker stations around the ring
- Each station has 8 tracking modules in the scalloped region in front of a calorimeter
- Each module has ~200 aluminized mylar straws with 15µm walls, 5mm in diameter, 12cm long. Wire is 50um at 1.8kV, 50:50 Ar:Ethane gas at 1atm

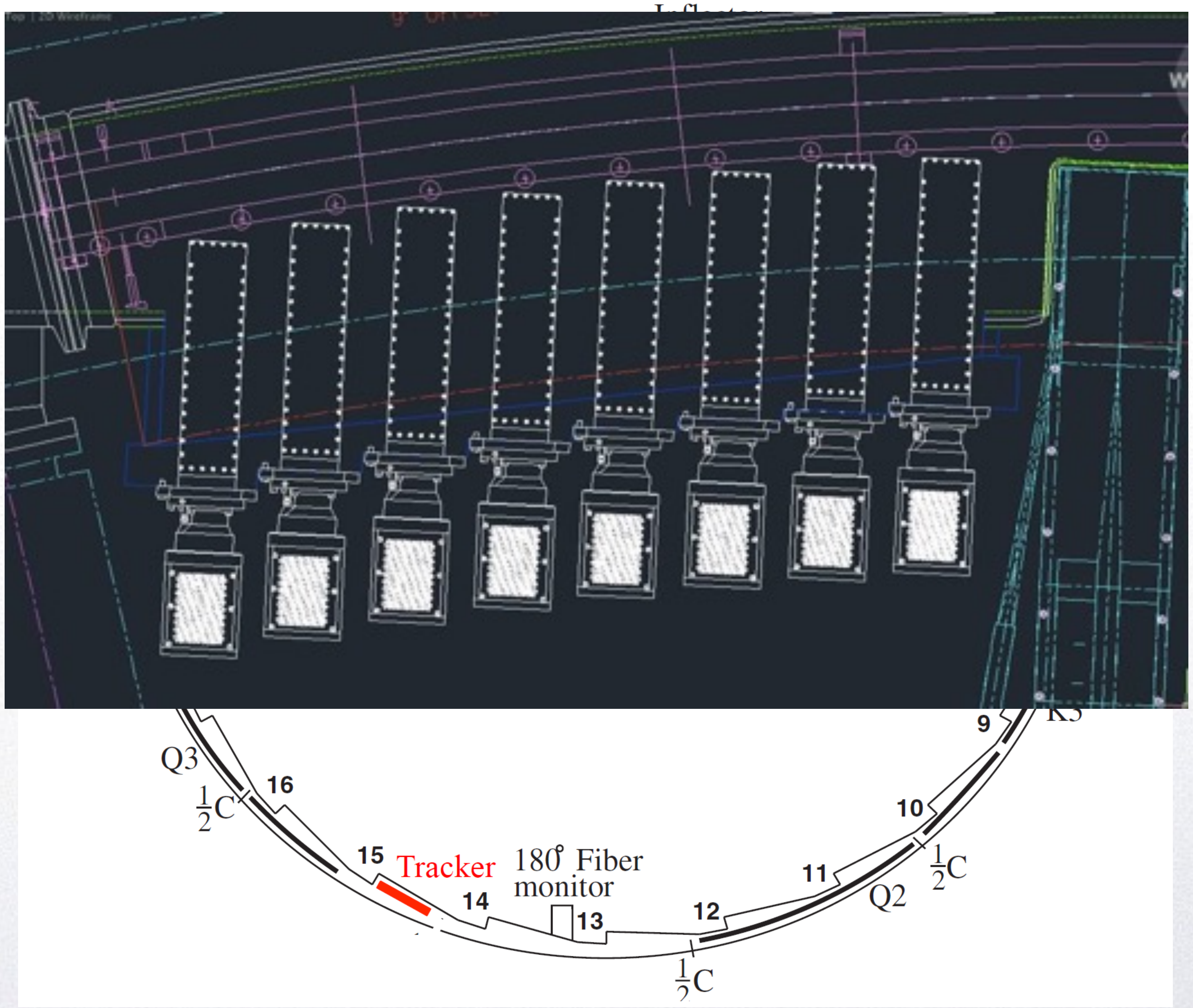

Straw Tube Trackers

- Three tracker stations around the ring
- Each station has 8 tracking modules in the scalloped region in front of a calorimeter
- Each module has ~200 aluminized mylar straws with 15µm walls, 5mm in diameter, 12cm long. Wire is 50um at 1.8kV, 50:50 Ar:Ethane gas at 1atm

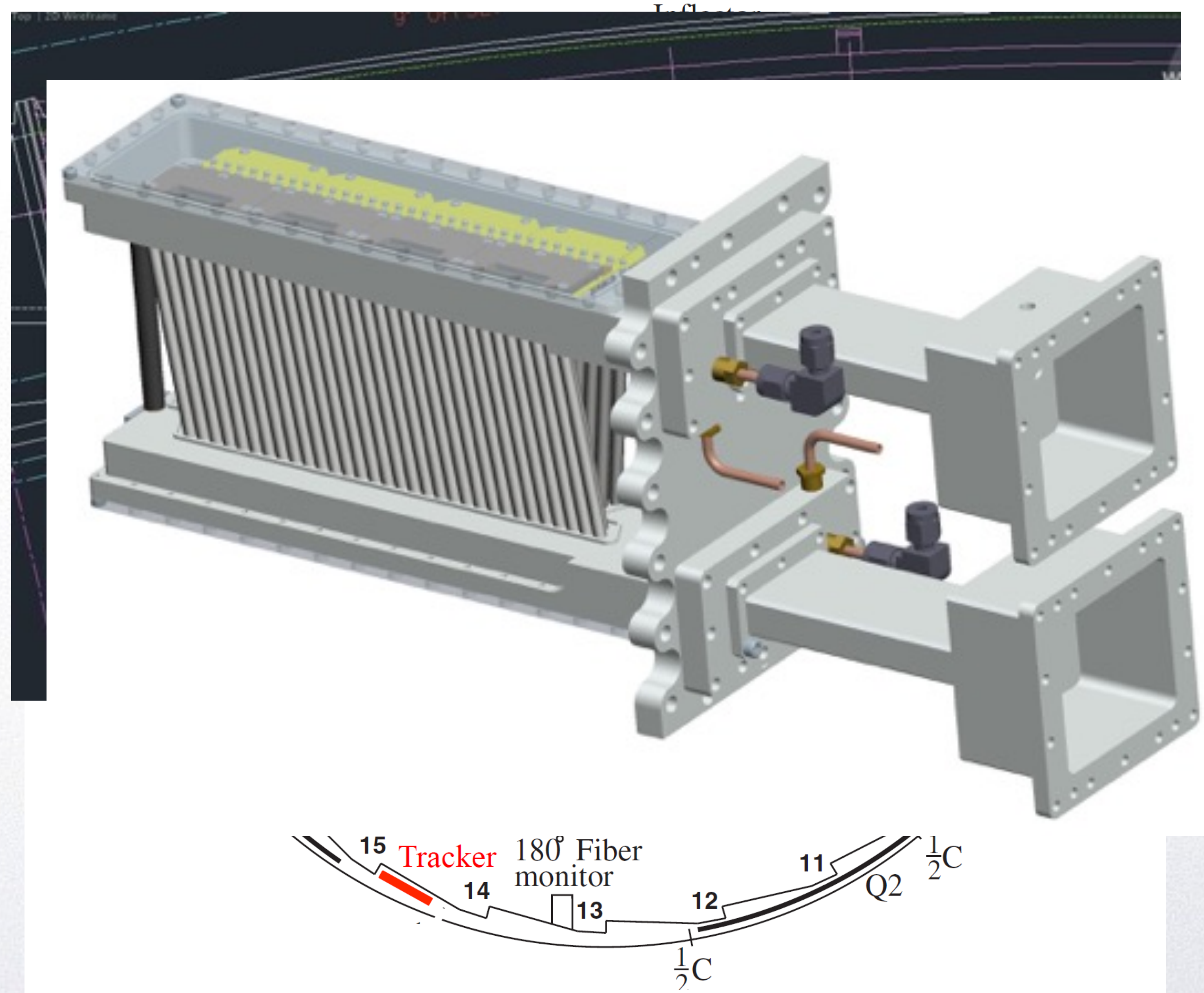

E-989 Schedule

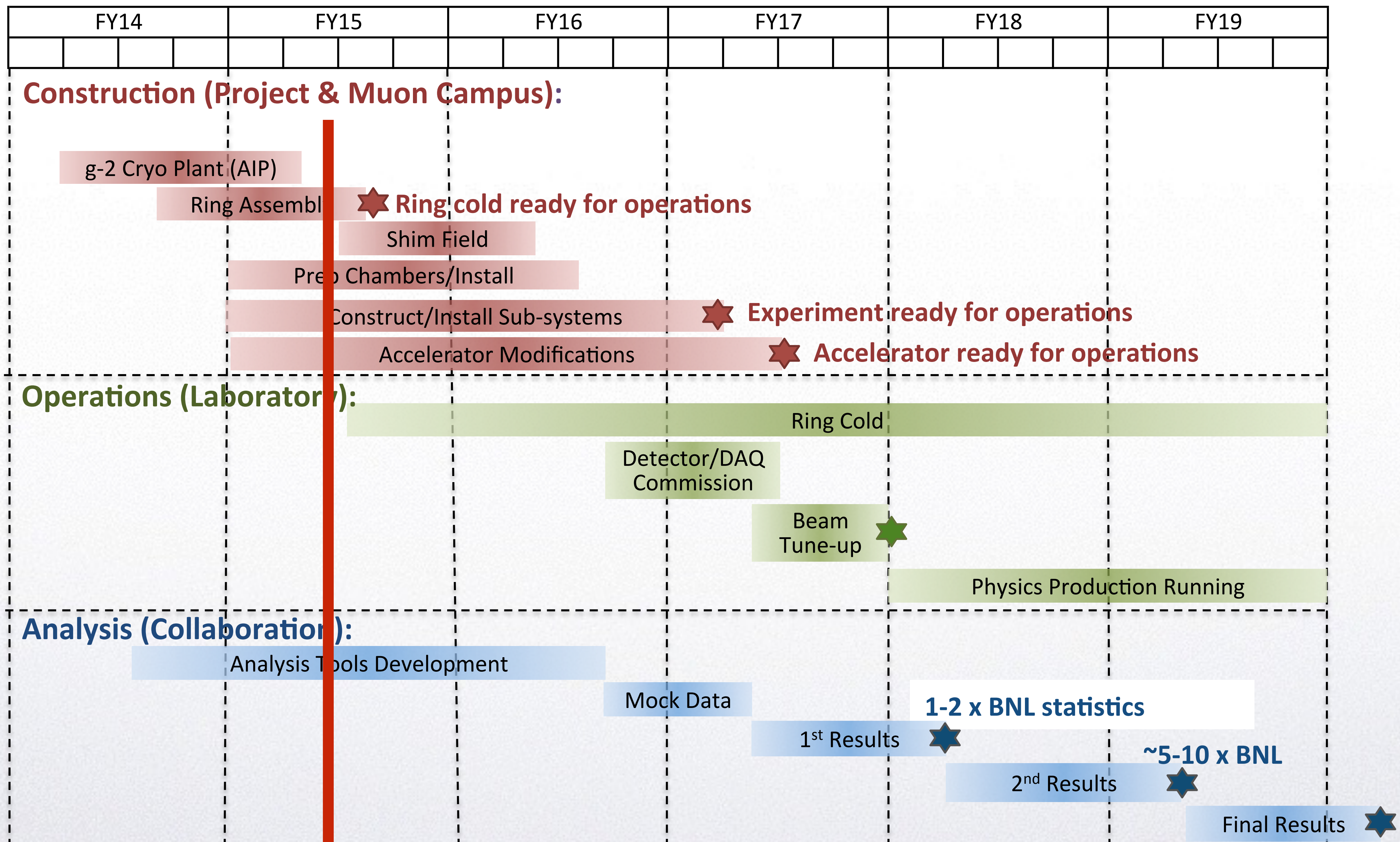

Schedule from C. Polly, project manager

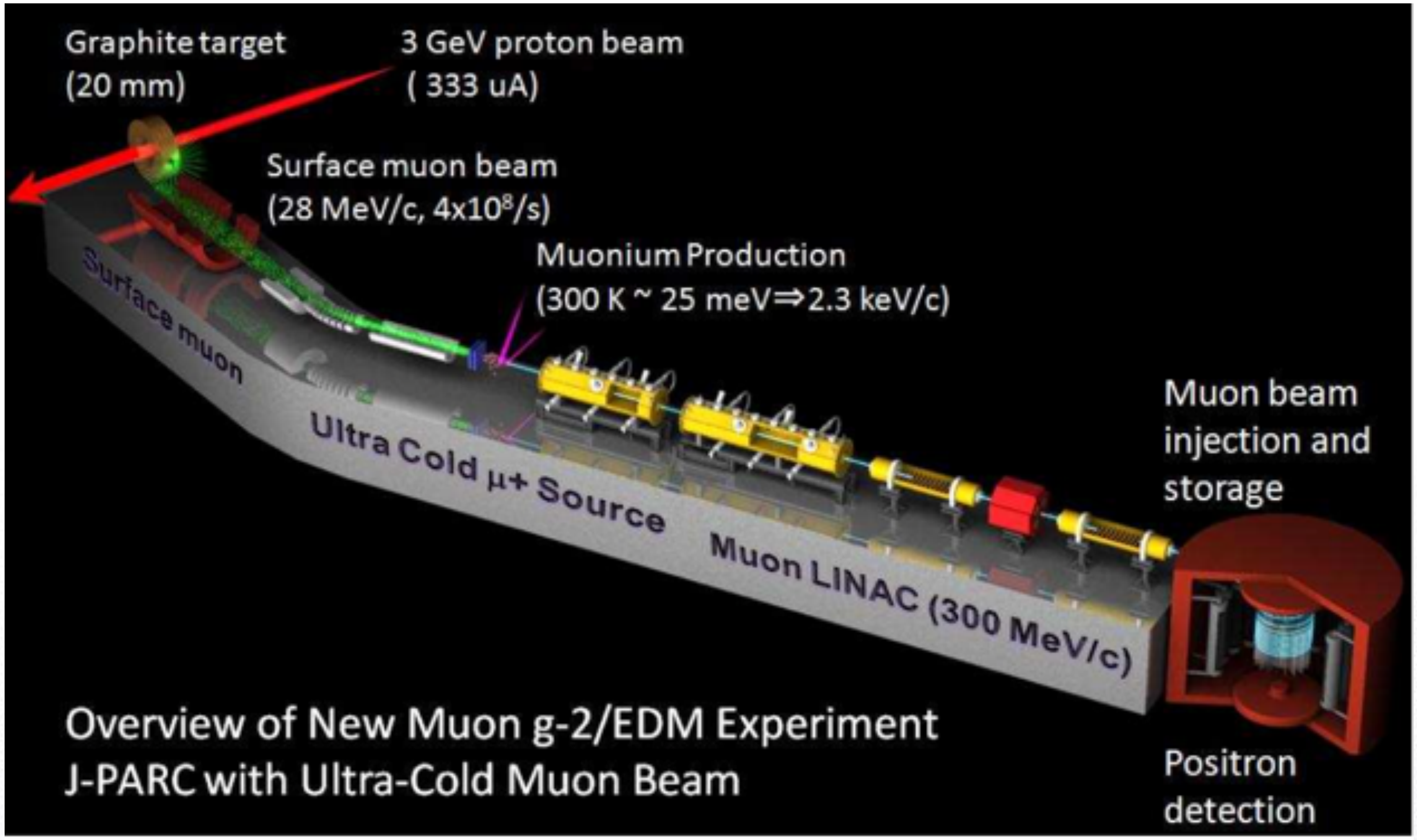
Graphite target
(20 mm)
3 GeV proton beam
(333 uA)
Surface muon beam
(28 MeV/c, 4x10⁸/s)
Muonium Production
(300 K ~ 25 meV⇒2.3 keV/c)
Surface muon
Ultra Cold μ+ Source
Muon LINAC (300 MeV/c)
Muon beam
injection and
storage
Positron
detection
Overview of New Muon g-2/EDM Experiment
J-PARC with Ultra-Cold Muon Beam

E-34 at J-PARC

Motivation

- Different (and very complementary) approach to Fermilab experiment
- If you start with muons with ~zero transverse momentum, you don't need any electric fields

$$\vec{\omega}_a = \frac{e}{mc}\left[a\vec{B} - \left(a - \frac{1}{\gamma^2 - 1}\right)\vec{\beta} \times \vec{E}\right]$$

- Experiment can then be much more compact

Motivation

- Different (and very complementary) approach to Fermilab experiment
- If you start with muons with ~zero transverse momentum, you don't need any electric fields

$$\vec{\omega}_a = \frac{e}{mc}\left[a\vec{B} - \left(a - \frac{1}{\gamma^2 - 1}\right)\cancel{\vec{\beta} \times \vec{E}}\right]$$

- Experiment can then be much more compact

Ultra-cold Muons

- Protons on graphite target produce polarized surface muons
- Muons stopped to form Muonium atoms, drift into vacuum
- Ionized with two lasers, accelerated with LINAC
- Produces beam of 300 MeV ultra-cold muons with 50% polarization

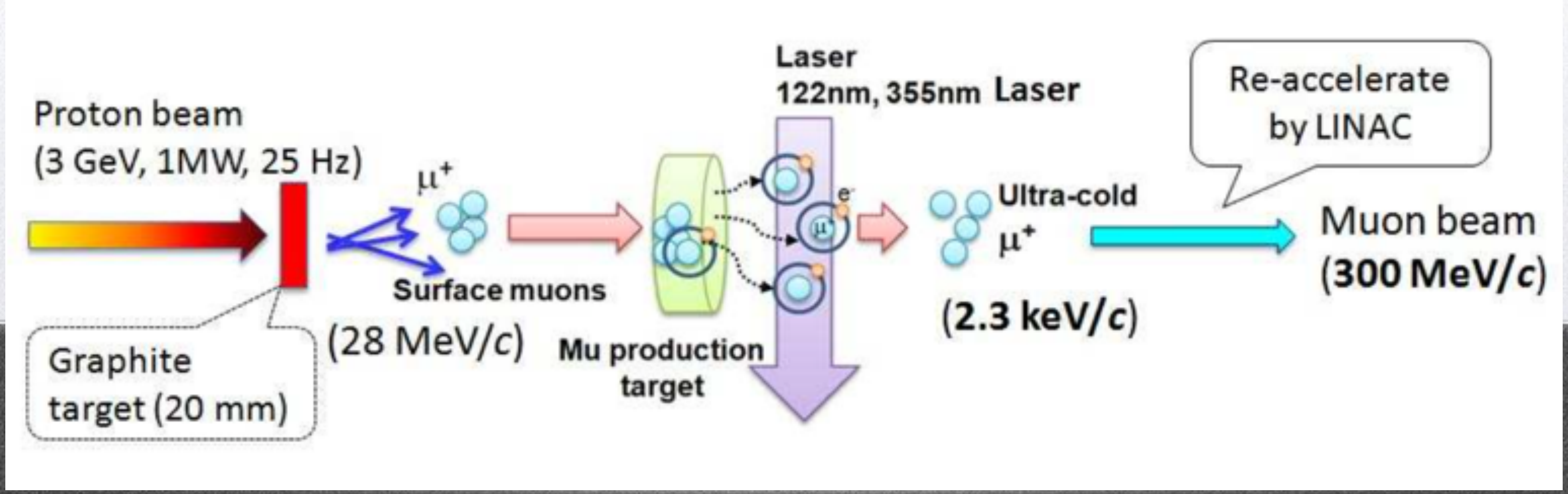

Muonium Production

- Limiting factor is diffusion of Muonium from room temperature source
- Recent successes at TRIUMF with silica aerogel with laser-ablated micro-channels
- Currently predicting total muon rate into g-2 detector of 0.2×10^6/s

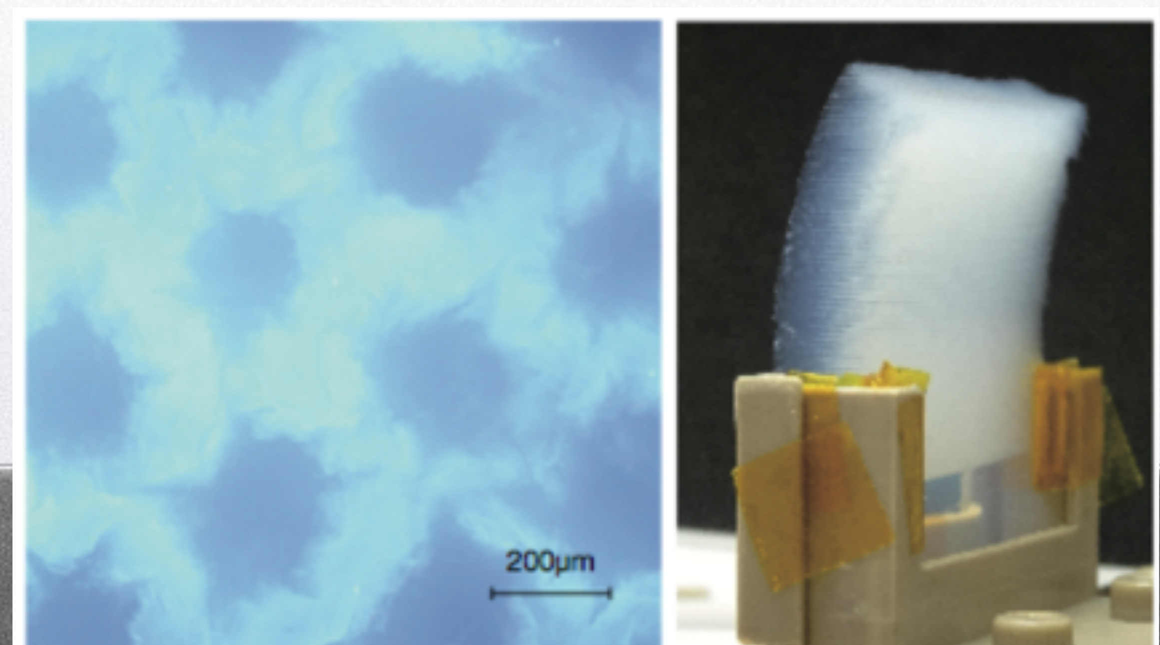

Prog. Theor. Exp. Phys. (2013)
arXiv: 1407.8248

Injection to Storage Ring

- 300 MeV muons injected into 3.0T, 33cm-radius solenoidal magnet
- Magnetic coils give kick to stabilize vertically
- Very weak magnetic focusing

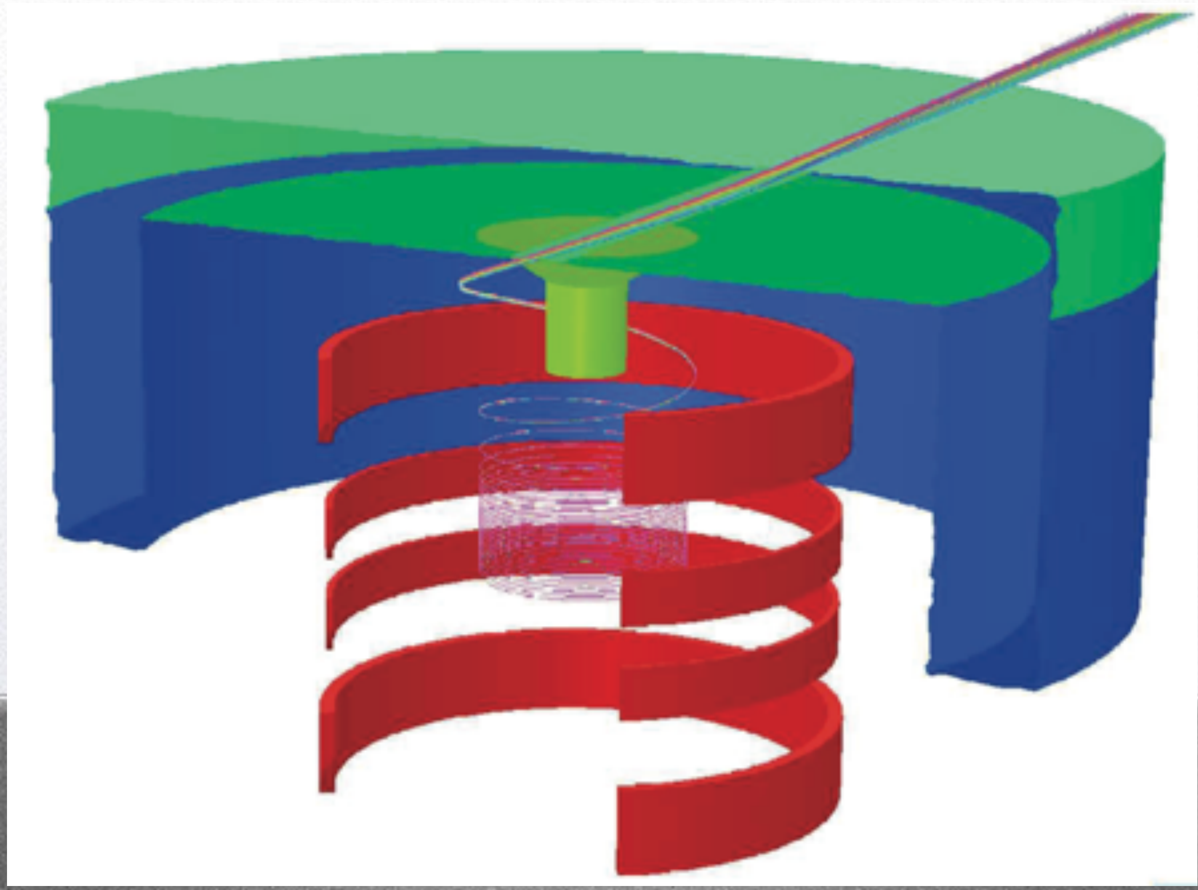

Injection to Storage Ring

- 300 MeV muons injected into 3.0T, 33cm-radius solenoidal magnet
- Magnetic coils give kick to stabilize vertically
- Very weak magnetic focusing

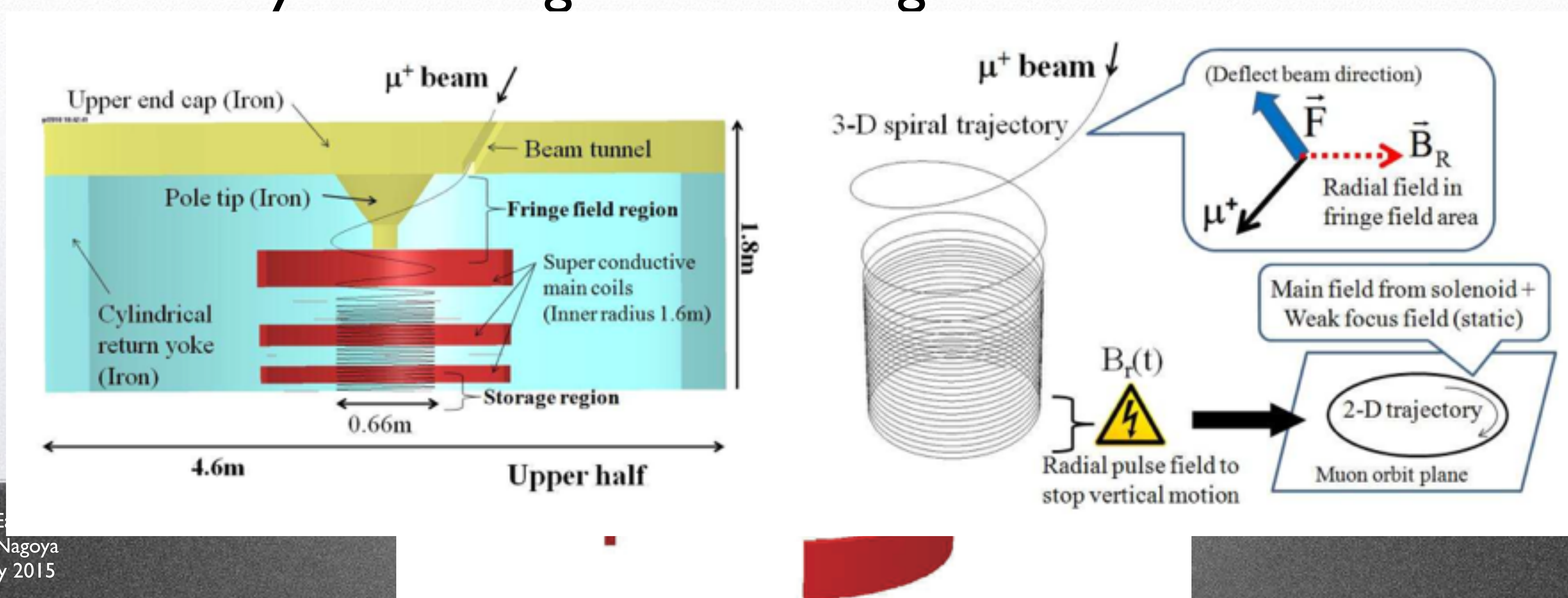

Detectors

- Double-sided silicon sensors inside of orbit, 200 µm pitch
- ~40 vanes, each 6cm in radius, 12cm in height
- Total of 98 planes, 691k strips
- E/B fields from detectors under study

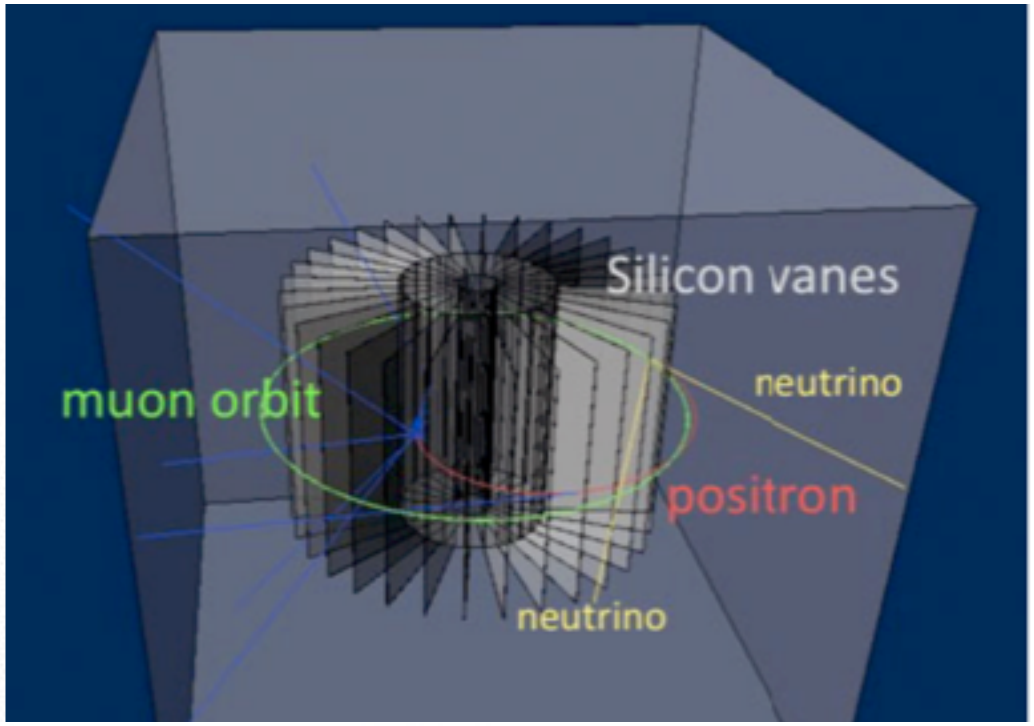

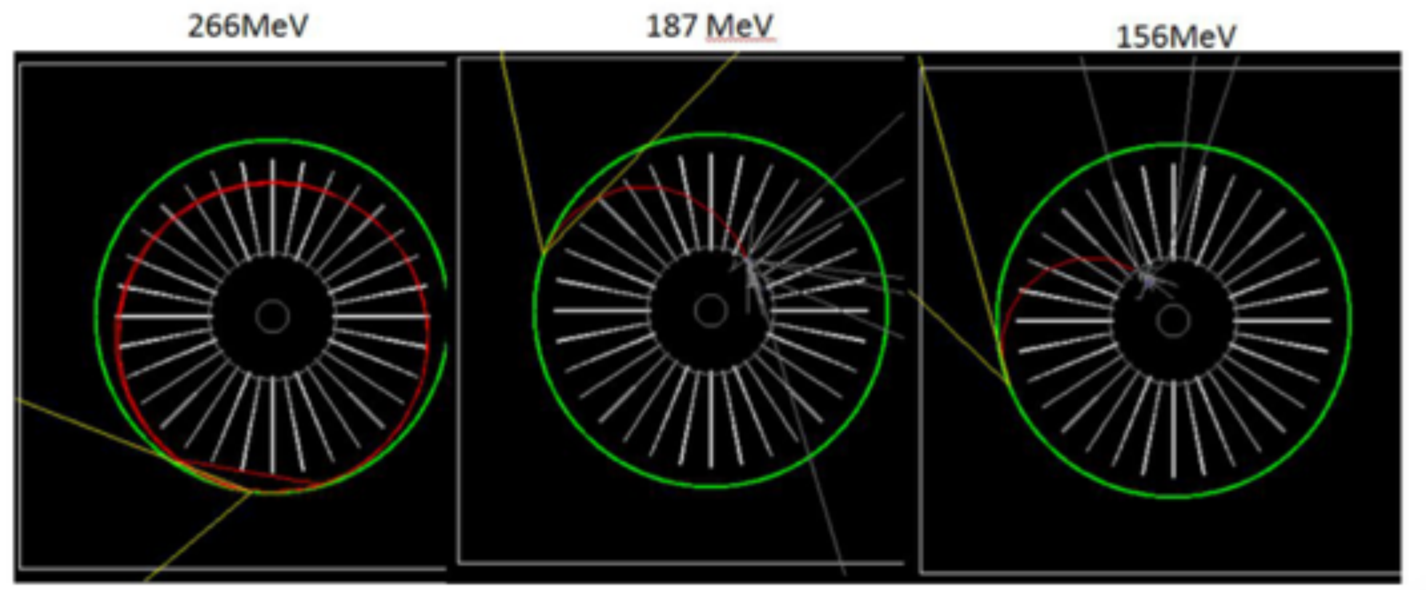

Figure 6: Example positron trajectories in the detector system at three different energies of positrons. The green circle is the muon beam orbit. The red trajectory is the trace of the positron track. The white tracks are photons.

Expected Results

- Aiming at comparable uncertainty (statistical and systematic) as Fermilab experiment
- Latest results on ultra-cold muon production extrapolates to 400ppm statistical uncertainty (instead of 100ppm)
- In any case, will be a crucial second measurement of the muon g-2

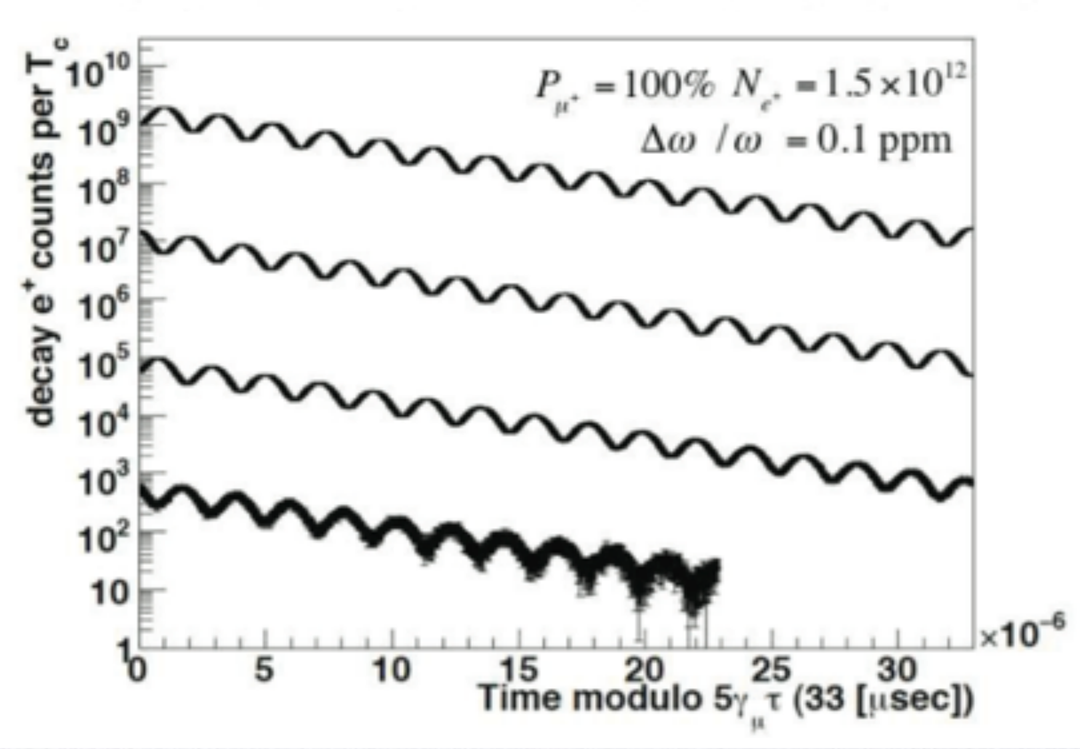

Comparison

Table 4: Comparison of various parameters for the Fermilab and J-PARC $(g-2)$ Experiments

Parameter	Fermilab E989	J-PARC E24
Statistical goal	100 ppb	400 ppb
Magnetic field	1.45 T	3.0 T
Radius	711 cm	33.3 cm
Cyclotron period	149.1 ns	7.4 ns
Precession frequency, ω_a	1.43 MHz	2.96 MHz
Lifetime, $\gamma\tau_\mu$	64.4 μs	6.6 μs
Typical asymmetry, A	0.4	0.4
Beam polarization	0.97	0.50
Events in final fit	1.8×10^{11}	8.1×10^{11}

Gorringe and Hertzog, Progress in Nuclear and Particle Physics, *to appear*

Electric Dipole Moments

- Muon EDM produces a tilt in the precession plane
- E-989 expects an order of magnitude improvement on current limit (1.8x10^{19} e cm) early in run
- E-34 expects another order of magnitude beyond this

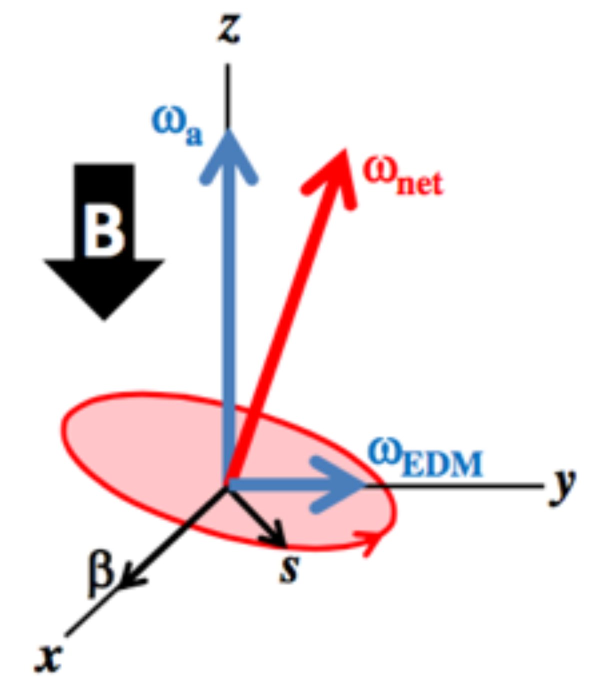

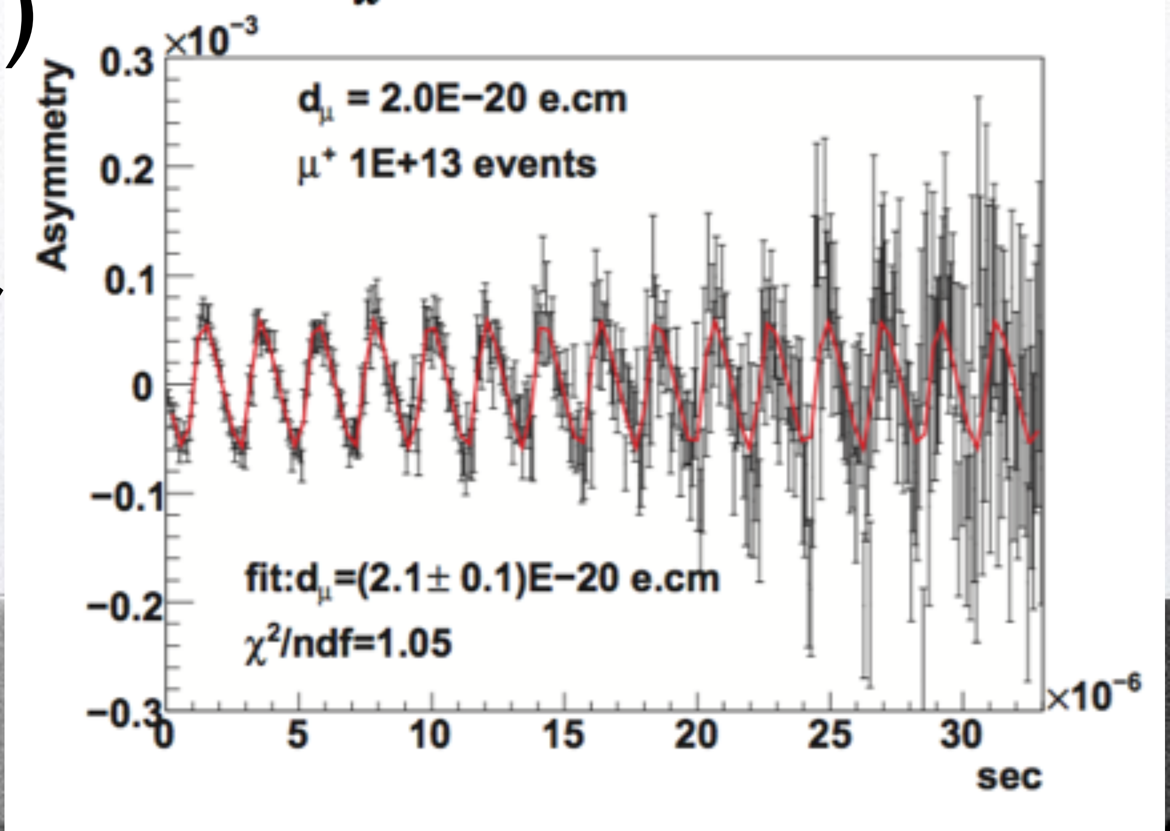

Conclusion

- The muon anomalous magnetic moment is one of best hints we have of new physics
  - The current best measurement (0.54ppm) shows a 3σ discrepancy with the SM
- The next generation experiments (E989 at Fermilab and E34 at J-PARC) will reduce the uncertainty by a factor of 4 in the next few years

Backup

New Physics

- Ultimately, any new particle coupling to muons would introduce new loop diagrams to the μ-μ-γ vertex, and hence change the value of the muon magnetic moment
- Lots of possibilities: Supersymmetric particles, dark photons, etc...
- In principle, can be sensitive to mass scales beyond what can be directly probed at the LHC

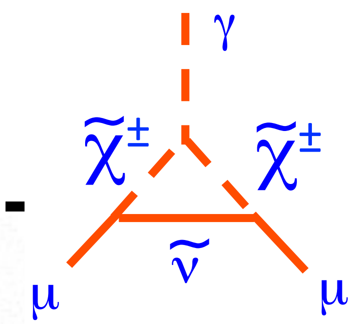

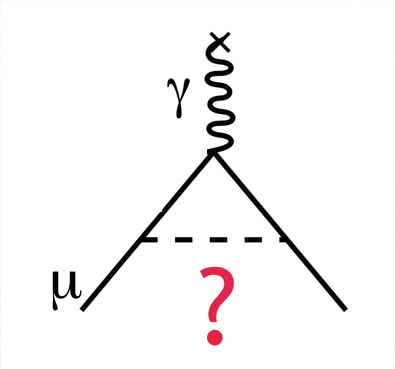

$$a_\mu = a_\mu^{QED} + a_\mu^{had} + a_\mu^{EWK} (+a_\mu^{NP}?)$$

SM Prediction

HVP

	$\delta(\sigma)/\sigma$ present	δa_μpresent	$\delta(\sigma)/\sigma$ future	δa_μfuture
$\sqrt{s} < 1$ GeV	0.7%	33	0.4%	19
$1 < \sqrt{s} < 2$ GeV	6%	39	2%	13
$\sqrt{s} > 2$ GeV		12		12
total		53		26

Table 2.4: Overall uncertainty of the cross-section measurement required to get the reduction of uncertainty on a_μ in units 10^{-11} for three regions of $\sqrt{s}$ (from Ref. [93]).

	VALUE ($\times 10^{-11}$) UNITS
QED ($\gamma + \ell$)	$116\,584\,718.951 \pm 0.009 \pm 0.019 \pm 0.007 \pm 0.077_\alpha$
HVP(lo) [71]	$6\,923 \pm 42$
HVP(lo) [72]	$6\,949 \pm 43$
HVP(ho) [72]	-98.4 ± 0.7
HLbL	105 ± 26
EW	153.6 ± 1.0
Total SM [71]	$116\,591\,802 \pm 42_{\text{H-LO}} \pm 26_{\text{H-HO}} \pm 2_{\text{other}}\ (\pm 49_{\text{tot}})$
Total SM [72]	$116\,591\,828 \pm 43_{\text{H-LO}} \pm 26_{\text{H-HO}} \pm 2_{\text{other}}\ (\pm 50_{\text{tot}})$

arXiv: 1501.06858

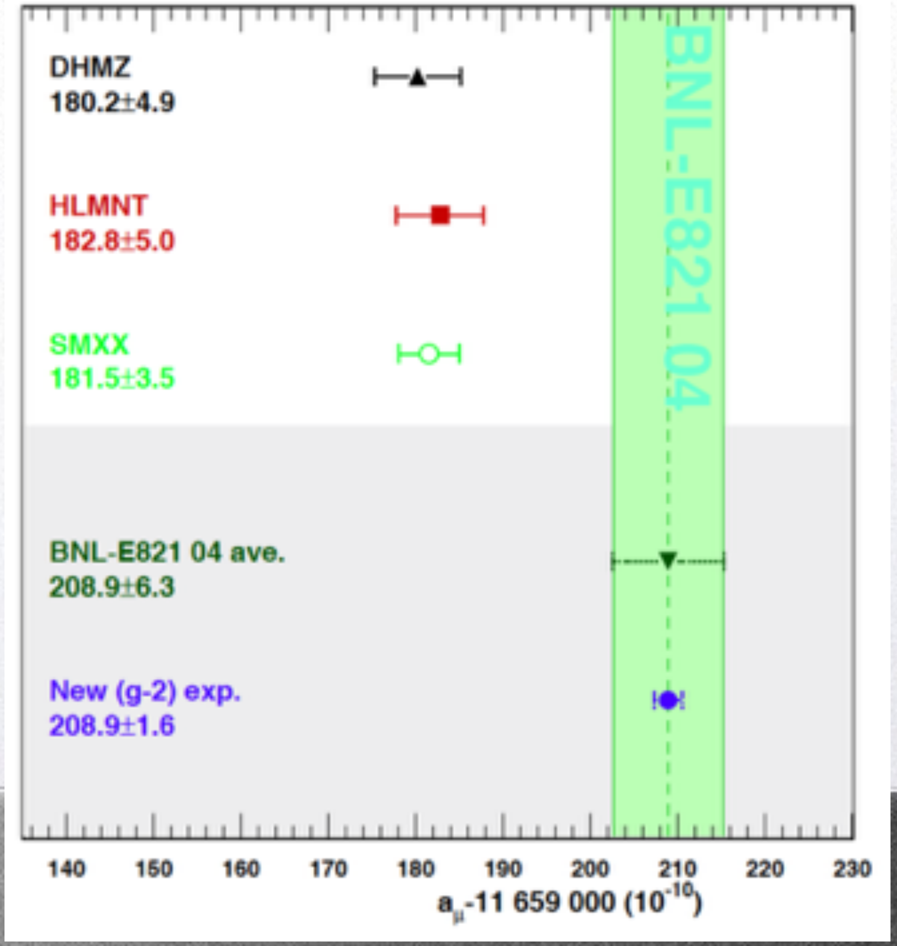

The Measurement

$$a_\mu = \omega_a \frac{mc}{eB}$$

Limited by precision on muon mass

$$a_\mu = \frac{\omega_a/\omega_p}{\lambda_+ - \omega_a/\omega_p}$$

Express magnetic field in terms of ω_p, Larmor frequency of free proton

λ_+ is ratio of muon to proton magnetic moment (known to 37ppb)

The Big Move

- Summer 2013: Successfully moved 50-ft wide superconducting coils from Brookhaven to Fermilab

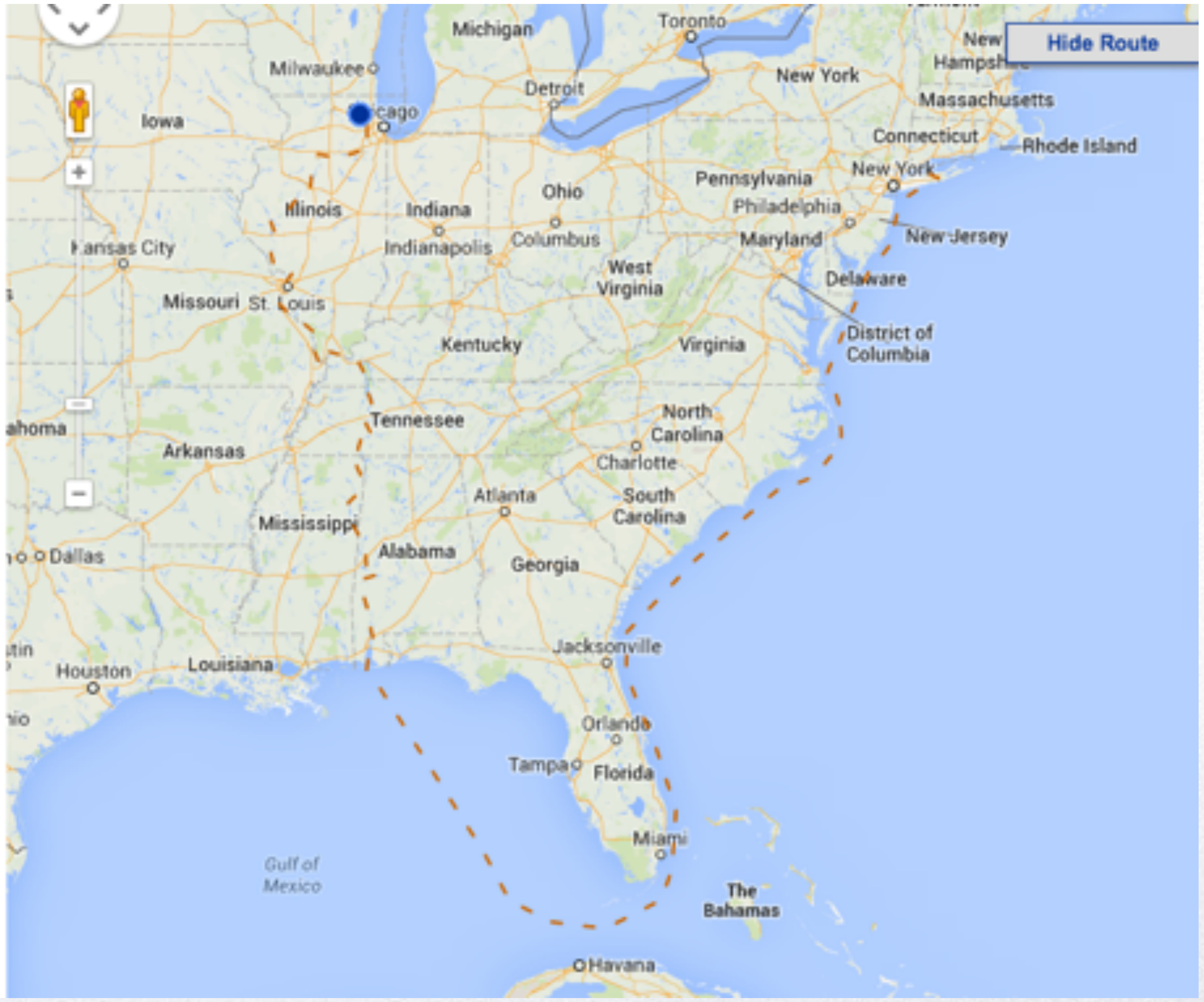

Making the Sausage...

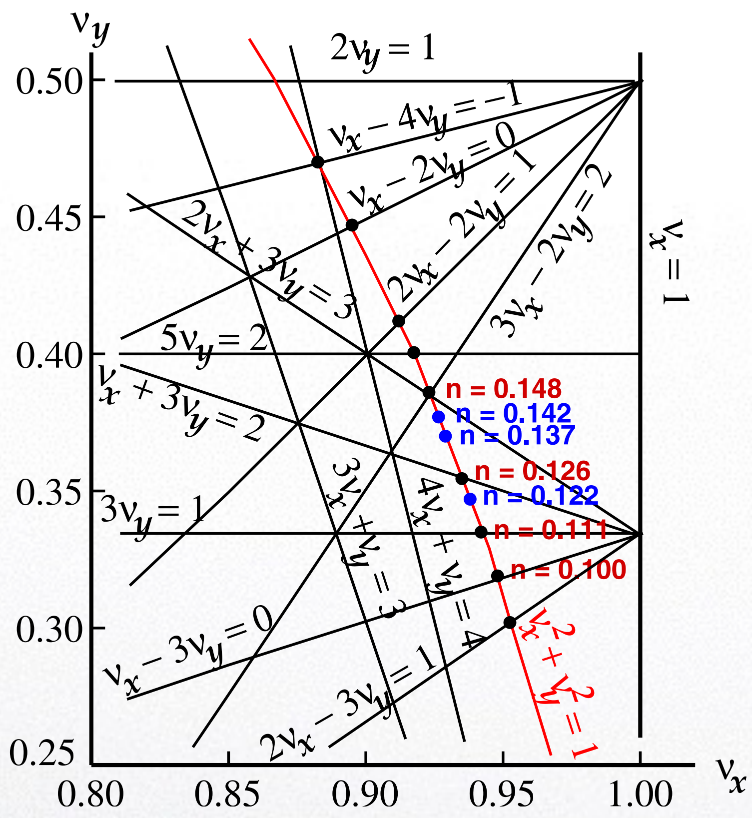

FIG. 18 (color online). The tune plane showing resonance lines. Three of the n values used to run the experiment, 0.122, 0.137, 0.142, are indicated on the arc of the circle defined as $v_x^2 + v_y^2 = 1$. They do not intersect any of the resonance lines, contrary to nearby tunes, which are also shown on the arc.

PHYSICAL REVIEW D **73,** 072003 (2006)

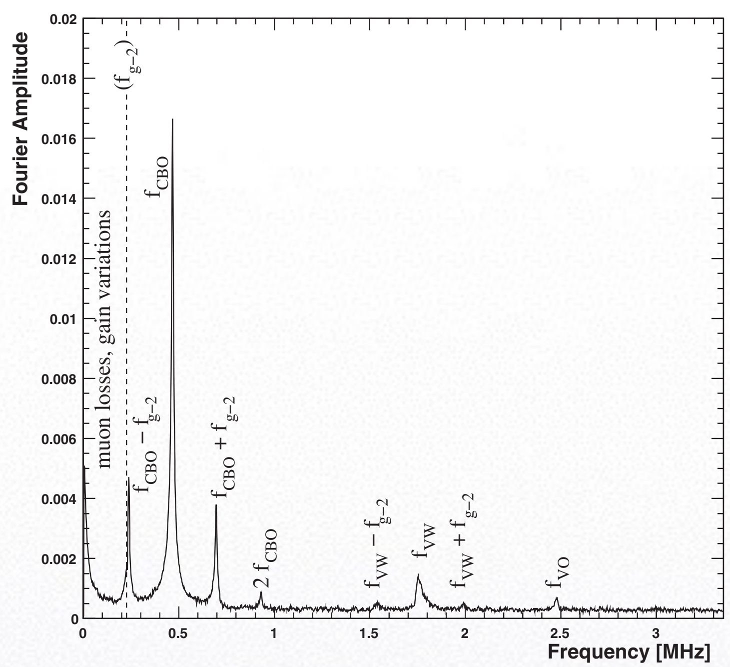

FIG. 34. The Fourier spectrum obtained from residuals from a fit based on the five-parameter, ideal muon decay and spin precession expression. The horizontal coherent betatron oscillation (CBO) frequency at 466 kHz, its first harmonic, and the difference frequency between CBO and the $(g - 2)$ frequency are strong peaks. The vertical waist (VW) and CBO vertical oscillation (VO) produce smaller, but still significant, effects at high frequencies. The low-frequency rise stems from muon loss and gain distortions of the underlying decay exponential.

TABLE VIII. Important frequencies and periods in the $(g - 2)$ storage ring for $n = 0.137$.

Physical frequency	Variable	Expression	Frequency	Period
Anomalous precession	f_a	$\frac{e}{2\pi m} a_\mu B$	0.23 MHz	4.37 μs
Cyclotron	f_c	$\frac{v}{2\pi R_0}$	6.71 MHz	149 ns
Horizontal betatron	f_x	$\sqrt{1-n} f_c$	6.23 MHz	160 ns
Vertical betatron	f_y	$\sqrt{n} f_c$	2.48 MHz	402 ns
Horizontal CBO	f_{CBO}	$f_c - f_x$	0.48 MHz	2.10 μs
Vertical waist	f_{VW}	$f_c - 2f_y$	1.74 MHz	0.57 μs